STYRELSEN FÖR

VINTERSJÖFARTSFORSKNING

WINTER NAVIGATION RESEARCH BOARD

Research Report No 123

Lars Axell, Tomas Landelius

BALTIC FORECAST IMPROVEMENTS USING REMOTE SENSING DATA

Finnish Transport and Communications Agency
Finnish Transport Infrastructure Agency
Finland

Swedish Maritime Administration
Swedish Transport Agency
Sweden

Talvimerenkulun tutkimusraportit — Winter Navigation Research Reports
ISSN 2342-4303
ISBN 978-952-311-793-8

FOREWORD

In this report no 123, the Winter Navigation Research Board presents the results of research project Baltic FIRE Baltic Forecast Improvements using Remote Sensing Data. The project incorporated more available satellite data than previously to improve the initial conditions for SMHI's operational ice-ocean forecast model to improve forecast quality.

The Winter Navigation Research Board warmly thanks Lars Axell and Tomas Landelius for this report.

Helsinki

June 2022

Lauri Kuuliala	Anders Dahl
Finnish Transport and Communications Agency	Swedish Maritime Administration
Jarkko Toivola	Stefan Eriksson
Finnish Transport Infrastructure Agency	Swedish Transport Agency

Baltic Forecast Improvements using Remote Sensing Data (Baltic FIRE): Final Report

Project number: W21-11 BalticFire

Authors: Lars Axell (Project leader) and Tomas Landelius,
Research and Development,
Swedish Meteorological and Hydrological Institute (SMHI),
Sweden

Date: 2021-11-30

Abstract

This project is the first part of a planned two-year project. The idea of the project is to start using more of the available satellite data in order to improve the initial conditions for our operational ice-ocean forecast models and thereby improving the forecast quality.

To this end, we have collected all relevant satellite data for our chosen target period December 2016 to May 2017. The data we collected include Sentinel-1 C-band Synthetic Aperture Radar backscatter as well as brightness temperature from the passive microwave AMSR2 instrument (several channels). We also simulated the whole target period with the operational NEMO-Nordic model, as well as with a similar setup covering only a small subdomain (the Bothnian Bay and the Bothnian Sea) to improve calculation speed, anticipating more demanding ensemble forecast simulations in the second part of the project.

The next step was to investigate several different methods of calculating model equivalents of the satellite radiances from both Sentinel and AMSR2. To be able to do this is key to being able to assimilate these data as envisioned in this project. Several so-called Radiative Transfer Models (RTMs) were investigated, including the Snow Microwave Radiative Transfer (SMRT) model and the Community Microwave Emission Modelling (CMEM) Platform, and also the statistical k Nearest Neighbor Regression (KNNR) method which is akin to a Machine Learning Method.

The main results so far is that the KNNR method gives best results for both Sentinel-1 C-SAR and AMSR2 data. In the future we will however spend more time on tuning both the physically based SMRT model and the KNNR method to improve the results further. The next steps in the second part of the project includes setting up an ensemble forecasting system for the ice-ocean model and start testing assimilating the satellite radiances.

1. Introduction

Today's ice ocean forecasts made at SMHI include the most important ice variables. However, to make good forecasts requires good initial conditions (the state that we start the model from), good boundary conditions (including meteorological forcing), and a good numerical model that can accurately calculate future states (a forecast). What we are lacking today is mainly the first criterion, i.e. a good initial condition. Without proper data assimilation, where we use observations to correct the initial conditions, it doesn't really matter much if the numerical model is good or not, if we start each forecast from a sea state with large errors. As a result, today's ice forecasts are of little use. Large areas covered with sea ice may be ice free in the forecast, and vice versa. Though the thermodynamics in the model is generally good from a climatological point of view, ice extent is challenging to forecast, because small errors in ocean heat content may lead to unacceptable errors in e.g. ice extent. This project is about increasing the use of remote sensing data (satellite data) with the goal of improving the initial states of ice-ocean forecasts, but also weather forecasts due to the loose coupling between the models.

Daily ice charts are available for ice assimilation, but they are created manually by ice analysts with some degree of subjectivity. Though the ice edge is usually well defined, the ice concentration and ice thickness both have large uncertainties. In addition, snow depth is not available from these charts. Further, in atmospheric data assimilation it is well established that direct assimilation of satellite data is preferable to assimilation of products which can result in inconsistencies.

In this project we have set out to start studying how to use satellite data (Sentinel-1 C-band synthetic aperture radar data and AMSR2 passive microwave data, both of which are rather insensitive to the state of the atmosphere) together with Radiative Transfer Models (RTMs) to compute model equivalents, i.e. what the satellite should observe given the ice-ocean model state. In this way we hope to, in the near future, be able to improve the constraint on the ice-ocean forecast model with respect to ice extent, ice concentration, ice thickness, sea surface temperature and possibly also snow depth on the ice.

2. Project plan

The Baltic FIRE project has been divided into two parts (henceforth called Baltic FIRE-1 and Baltic FIRE-2, respectively), and in this year's contract (Baltic FIRE-1) the following work was planned (list of work package descriptions and briefly what we have done):

Work Packages (Wps):

WP0: Administration and dissemination (1 month

The dissemination during BALTIC FIRE-1 has so far been restricted to the writing of the Final Report and giving an oral presentation at the Baltic Operational Oceanographic System (BOOS) Annual Meeting, on November 25, 2021, with the title "Direct assimilation of satellite radiances into NEMO: Status from an ongoing project".

WP1: Data and software collection (0.5 months)

Sentinel-1 C-band SAR data as well as AMSR2 data were downloaded for the target period (December 2016 to May 2017) and stored at Nationellt Superdatorcentrum (NSC; https://liu.se/organisation/liu/nsc), used by SMHI for computing-intensive calculations and storage of data. The Snow Microwave Radiative Transfer (SMRT, Picard et al., 2018) model as well as RTTOV (Radiative Transfer for TOVS including FASTEM, Saunders et al., 2020) and CMEM (The Community Microwave Emission Modelling Platform, de Rosnay et al., 2019) were downloaded and installed at NSC. The idea was to model snow and ice properties with SMRT (for both Sentinel-1 C-SAR and AMSR2), the contribution from open sea with FASTEM or CMEM for AMSR2 and with an empirical function for Sentinel (instead of more complicated physical models like the M4S software (Romeiser & Thompson, 2000) and the DopRIM model (Kudryavtsev et al., 2005). Empirical models have previously been employed successfully to wind speed retrievals using "geophysical model functions" (GMFs) relating sea surface characteristics to radar backscatter. Here we decided to try k-nearest neighbour regression (KNNR) to obtain a simple empirical (statistical) model for the Sentinel-1 C-SAR backscatter (class sklearn.neighbors.KNeighborsRegressor in Scikit-learn, Pedregosa et al., 2011). KNNR can be seen as a machine learning approach where the target is predicted by local interpolation of the targets associated with the nearest neighbors in the training set (. It turned out that this approach outperformed the physical models regarding snow, ice as well as open water for both AMSR2 and Sentinel-1 C-SAR. More on this in the results section.

AMSR2 (Advanced Microwave Scanning Radiometer - 2) is a microwave (MW) imager with 7 frequencies / 16 window (surface sensitive) channels ranging from 6.9 to 89 GHz with horizontal and vertical polarization. It has global coverage once a day and employs a conical scanning technique (55° zenith angle) with a 1450 km swath and pixel size of 10 km and an instantaneous field of view (IFOV, i.e. the solid angle through which the detector is sensitive to radiation) that is frequency dependent, see Table 1. In this project we skipped the 89 GHz channels due to their sensitivity to precipitation.

Table 1. Center frequencies (Freq), NEDT (noise equivalent differential temperature - the temperature difference which would produce a signal equal to the temporal noise) and IFOV (cross track x along track).

Freq (GHz)	6.925	7.3	10.65	18.7	23.8	36.5	89.0A	89.0B
NEDT (K)	0.3	0.3	0.6	0.6	0.6	0.6	1.1	1.1
IFOV (km)	35 x 62	35 x 62	24 x 42	14 x 22	11 x 19	7 x 12	3 x 5	3 x 5

For convenience we used the AMSR2 L1R product where the measurements from the lower frequency channels are resampled and reweighted to match the positions of the measurements for the 89A channels. The AMSR2 L1R product was read and calibrated with the pytroll software (https://pytroll.github.io/).

Sentinel-1 C-SAR is an all-weather multi-purpose synthetic aperture radar (SAR) imager with global coverage every 5-6 days. The scanning technique is side-looking, 15-45° off-nadir and the center frequency is at 5.405 GHz, NESZ (Noise Equivalent Sigma Zero), σ^{o} = -25 dB and a radiometric accuracy of 1 dB (3 σ). It has multi-polarisation and variable swath/resolution in a number of different modes, see Table 2. Here we used data from the coarsest EW mode and its Level-1 Ground Range Detected (GRD) product. It consists of focused SAR data that has been detected, multi-looked and projected to ground range using an Earth ellipsoid model. Phase information is lost. The resulting product has approximately square spatial resolution pixels and square pixel spacing with reduced speckle at the cost of worse spatial resolution. The grid spacing of the NEMO model, approximately 1.85 km, is still two orders of magnitude coarser.

Table 2. Characteristics of the different scanning modes for the Sentinel-1 C-SAR.

Mode	Stripmap (SM)	Interferometric wide-swath (IW)	Extra-wide swath (EW)	Wave (WV)
Resolution (m)	4 x 5	5 x 20	25 x 80	20 x 5
Swath (km)	80	240	400	20 x 20

The Sentinel data was also read and processed (calibrated) with the pytroll software. Note that there are occasions when there is thermal noise in parts of the SAR images (mainly in the outermost of the five vertical stripes constituting the multi-looked EW mode). This noise could be reduced by further processing but was not done here. An example of the noise pattern is given in Figure 1.

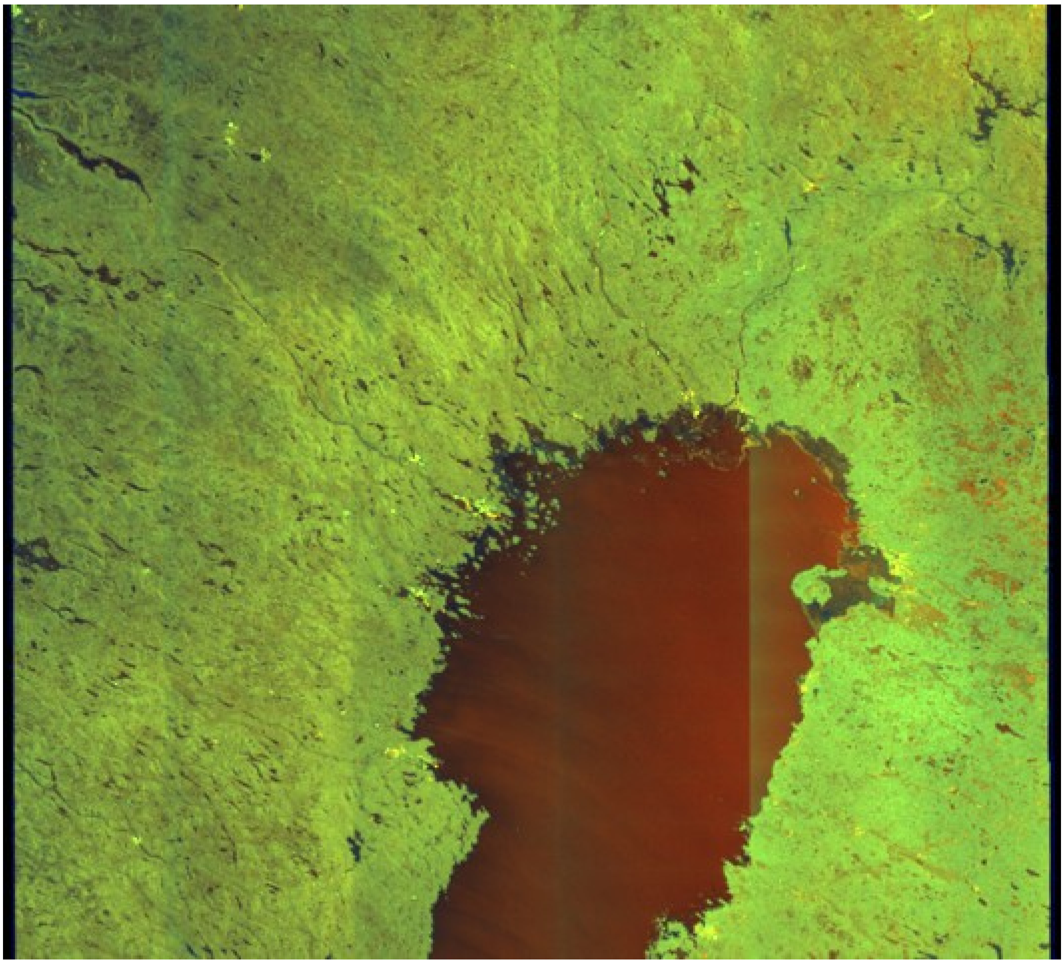

Figure 1. Example of SAR image with thermal noise in the rightmost strip.

WP2: Run the ice-ocean model for the target period (0.5 months)

The existing ice-ocean model setup NEMO-Nordic (e.g. Pemberton et al., 2017; Hordoir et al. 2019) was set up and used for simulating the target period. However, anticipating the future need for a faster setup, we decided to also test a very similar NEMO-based ice-ocean model setup, covering only Bothnian Sea and Bothnian Bay. The reduced domain covers the most important part of the satellite data downloaded in WP1 but has an open boundary in the Åland and Archipelago Seas (near latitude 59.9 degrees North); see Figure 2. As the two model setups gave similar results, we decided to use output from the faster one, the one with the smaller domain given in Figure 2, for the experiments described below.

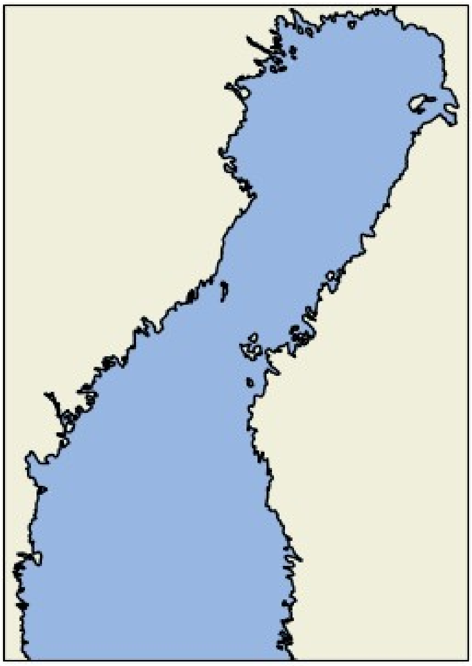

Figure 2. The region covered by the NEMO ocean model used in the project.

The following NEMO variables were saved from the model run every hour and made available as input for the RTM modelling in WP3: sea surface temperature, sea surface salinity, ice fraction, mean ice temperature, ice thickness, ice surface temperature, mean ice salinity, brine volume, snow temperature, snow thickness, and u- and v components of the 10 m wind.

Besides the above mentioned data we also downloaded parts of the world digital elevation model from the U.S. Geological Survey (GTOPO30) for use as a land-sea mask. GTOPO30 is a global raster digital elevation model (DEM) providing terrain elevation data with a horizontal grid spacing of 30 arc seconds (approximately 1 kilometer).

WP3: Develop new observation operator for satellite data (5 months)

As the planned duration time of this work package indicates, this was the most time consuming and demanding work package. For both the Sentinel-1 C-SAR and AMSR2 satellite data the task was to produce ice-ocean model equivalents for areas with open sea, ice and snow covered ice.

First the data was resampled and collocated in order to make comparisons on a common scale. For AMSR2 the NEMO data was resampled using gaussian weighting functions with a width matching the largest IFOV extent in Table 2. Separate weightings were done for open sea and ice based on the ice fraction. Hence we ended up with one set of NEMO variables for open sea; sea surface temperature and salinity along with u- and v components for the wind and one set for the ice part involving all the NEMO parameters. Moreover, only AMSR2 points for which the gaussian IFOV contained more than 95 % water (according to GTOPO30) were considered as valid for further comparisons.

In the Sentinel case it was the other way round and the Sentinel data was aggregated to represent the mean value within a NEMO grid box (ca 1.85 x 1.85 km). Here only Sentinel measurements representing water points, according to GTOPO30, were included in the average. The reason for this was that NEMO grid values only represent the water fraction of a grid box. Hence, the corresponding satellite data should refer to water points only.
A number of different radiative transfer model combinations were then fed with this collocated NEMO data and evaluated as summarized in Table 3. It turned out that applying KNNR to all surfaces was the most successful approach. The details are given in the results section.

Table 3: Model combinations applied to different surfaces. Yellow text: models applied only to AMSR2 data. Green text: models applied to both AMSR2 and Sentinel-1 C-SAR data.

RTM combination	#1	#2	#3	#4	#5
Sea	CMEM	CMEM	FASTEM	KNNR	KNNR
Ice	CMEM	SMRT	SMRT	SMRT	KNNR
Snow	CMEM	SMRT	SMRT	SMRT	KNNR

Milestones (M):

The project consists of the following milestones (M), all of which have been reached (planned project month within parentheses):

M1 (1): Radiative transfer model obtained. Satellite data retrieved for the time period December 2016 to May 2017.

M2 (2): The run with the ice-ocean model NEMO-Nordic of the target period is completed.

M3 (6): RTM set up for Sentinel-1 and AMSR-2. Data flow in place to feed the RTM with necessary ice-ocean model information.

M4 (10): Validation in terms of statistics for the departures between RTM simulations and satellite observations performed.

As noted above, the ocean model we ended up using is the reduced-domain version of NEMO-Nordic, which is expected to have similar performance except for being much faster to run.

Deliverables (D):

D1: Final report.
This is the Final Report for Baltic FIRE-1.

In the planned follow-up project, Baltic FIRE-2, we intend to further improve the observation operator using experience from Baltic FIRE-1 (BF2-WP1), in conjunction with the setup and tests with a new ensemble forecast system (BF2-WP2). The system will then be tested in a set of data assimilation experiments (BF2-WP3).

3.Results

In this section we summarize the results of the work in all Work Packages. First we present the major results concerning the evaluation of the RTMs for NEMO model equivalents to the Sentinel-1 C-SAR and AMSR2 measurements. Then we look at some findings regarding the different RTM models in more detail, e.g. regarding sensitivities to their input parameters and their performance compared to each other.
For brevity we use shorter notations for the variable names in the tables to follow. These are summarized in Table 4.

3.1 Major results

Best results obtained so far were obtained using the statistical KNNR method on the Sentinel-1 C-SAR data. The KNNR method also performs well on the AMSR2 data but only for the higher frequency channels where the IFOV is small enough to provide us with data from both open water and ice covered surfaces (in the Bay of Bothnia).
NEMO data were used together with standard values of some snow/ice properties and satellite viewing angle to calculate model equivalents of Sentinel-1 C-SAR backscatter and AMSR2 brightness temperatures.

Figure 3 below shows the first guess ice fraction for the sample date 2017-02-11, together with ice fraction from the ice chart from the same date, analyzed by the Swedish Ice Service at SMHI. It is clear that in this case the NEMO model overestimates the ice extent.

The top row of Figure 4 shows the backscatter for the two polarizations HH and HV, according to Sentinel-1 C-SAR observations as well as the model equivalent using the KNNR method. Though thermal noise is present in the observed HV polarization mode, it is clear that the model equivalents have responded to the presence of ice, though the backscatter depends on other parameters as well such as snow depth and ice thickness.

The bottom row of Figure 4 illustrates the observed and modelled (KNNR) brightness temperatures for the AMSR2 channels at 36.5 GHz. Again one can observe that the presence of ice in the NEMO model is reflected in the AMSR2 model equivalents.

Table 4. Explanation of variable names

Variable or parameter	Explanation
h_{snw}	Thickness of snow layer
t_{snw}	Temperature of snow layer
d_{snw}	Density of snow layer
l_{snw}	Correlation length of snow
h_{ice}	Thickness of ice layer
f_{ice}	Fraction of ice
ts_{ice}	Ice surface temperature
t_{ice}	Ice mean temperature
s_{ice}	Ice mean salinity
r_{ice}	Ice brine radius
p_{ice}	Porosity of ice
b_{ice}	Brine volume
ice type	Ice type in SMRT (“fresh ice” or “first-year ice”)
stickiness	Parameter in the microstructure model for ice and snow
t_{oce}	Temperature of ocean layer
s_{oce}	Salinity of ocean layer
u, v	Eastward and northward components of the wind
sat_{az}	Azimuth angle of satellite
sat_{el}	Elevation angle of satellite

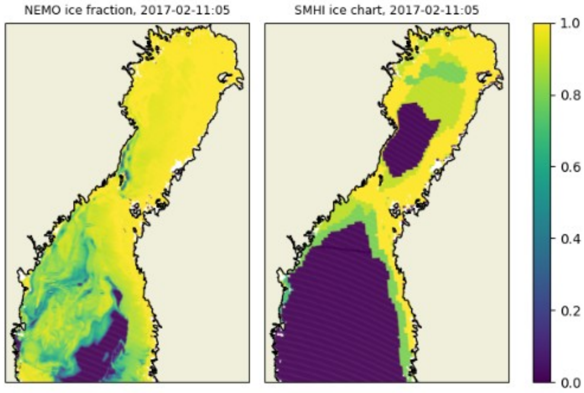

Figure 3. Ice fraction for the date 2017-02-11, according to (left) first guess from NEMO and (right) the ice chart from the Swedish Ice Service at SMHI.

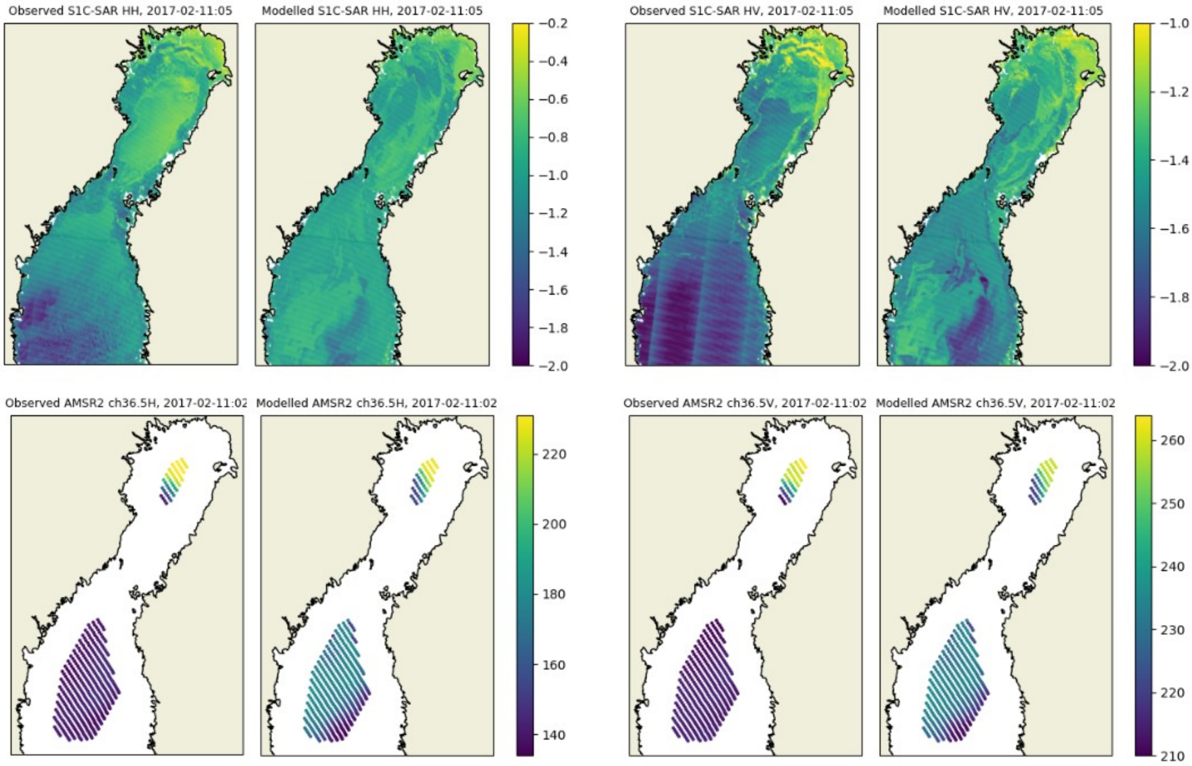

Figure 4. Examples of model equivalents for the date 2017-02-11.Top: Observed and calculated (KNNR) backscatter (dB) from Sentinel-1 C-SAR for (left) polarization HH and (right) polarization HV. Bottom: Observed and calculated (KNNR) brightness temperatures (K) for AMSR2 ch 36.5 for (left) polarization H and (right) polarization V.

These are exactly the results that we were hoping for, because now that we have a method to calculate model equivalents of the backscatter and brightness temperature observations, it will now be possible to assimilate these observations in our 3D/4D EnVar data assimilation system (Axell and Liu, 2016; 2017). This will be tested in the follow-up project Baltic FIRE-2.

To be able to use the information available also in the low-resolution AMSR2 data, we applied the same techniques as in the case of Sentinel-1 C-SAR data. However, as expected, with the large footprint of the AMSR2 data we could only analyze data that were far away from the coasts, which for all but the two highest frequency channels excluded all of the ice in the Bothnian Bay and almost all ice in the Bothnian Sea. Thus, with so little training data for ice covered waters, the KNNR method didn't provide any results for the AMSR2 channels at 6.925, 7.3 and 10.7 GHz.. Therefore, we plan to extend the test period to include many days with much more ice in the Bothnian Sea, to use as a learning data set for the KNNR method (the winter 2017/2018 is a good candidate, being a "normal" ice winter with more ice in the Bothnian Sea). In this way we will be able to use the information also in the AMSR2 data.

3.2 Modelling Sentinel-1 C-SAR backscatter

The SMRT model can model the Sentinel-1 C-SAR backscatter over areas with ice and snow. For the open sea we have so far avoided complicated physical models like M4S and DopRIM (mentioned in section 2) and instead employed simpler empirical models.
Hence we started out by modelling the ice and snow covered parts with SMRT using the information available from the NEMO model. However, there were a number of parameters that were not available and therefore had to be set to reasonable values based on suggested default values in the SMRT documentation or litterature, see Table 5.

Table 5. Surface related variables needed as input to the SMRT RTM. Green: Available from NEMO. Red: Not available from NEMO, constant values used indicated. Besides the entities in the table also ice type needs to be specified. In the simulations it was set to first year ice.

	Temp	Salinity	Thickness	Density	Brine vol	Brine radius	Stickiness	Corr length
Snow	x		x	x 350 g/m3				x 100 um
Ice	x	x	x	x 900 g/m3	x	x 0.2 mm	x 0.2	
Water	x	x						

The probability distribution (PDF) of the backscatter modelled with SMRT turned out to be quite different from the one representing the measured backscatter. In order to compensate for this we employed a CDF (cumulative distribution function) matching technique known as quantile mapping (QM, Panofsky and Brier, 1968). This allows us to map the modelled value onto a new one such that its PDF (and CDF) matches the one of the measurements.
For the open sea part we tested a simple Machine Learning (ML)/statistical approach known as KNNR. Here the modelled value is given as a weighted (e.g. inverse distance) average of the outputs associated with the K nearest neighbours to the input vector. Out of curiosity we also applied the KNNR method to the case with ice and snow and it turned out that it outperformed the physical SMRT model, see the error statistics presented in Table 6 and Figure 5. Here the KNNR estimates for water and ice surfaces were weighted together according to the NEMO ice fraction.

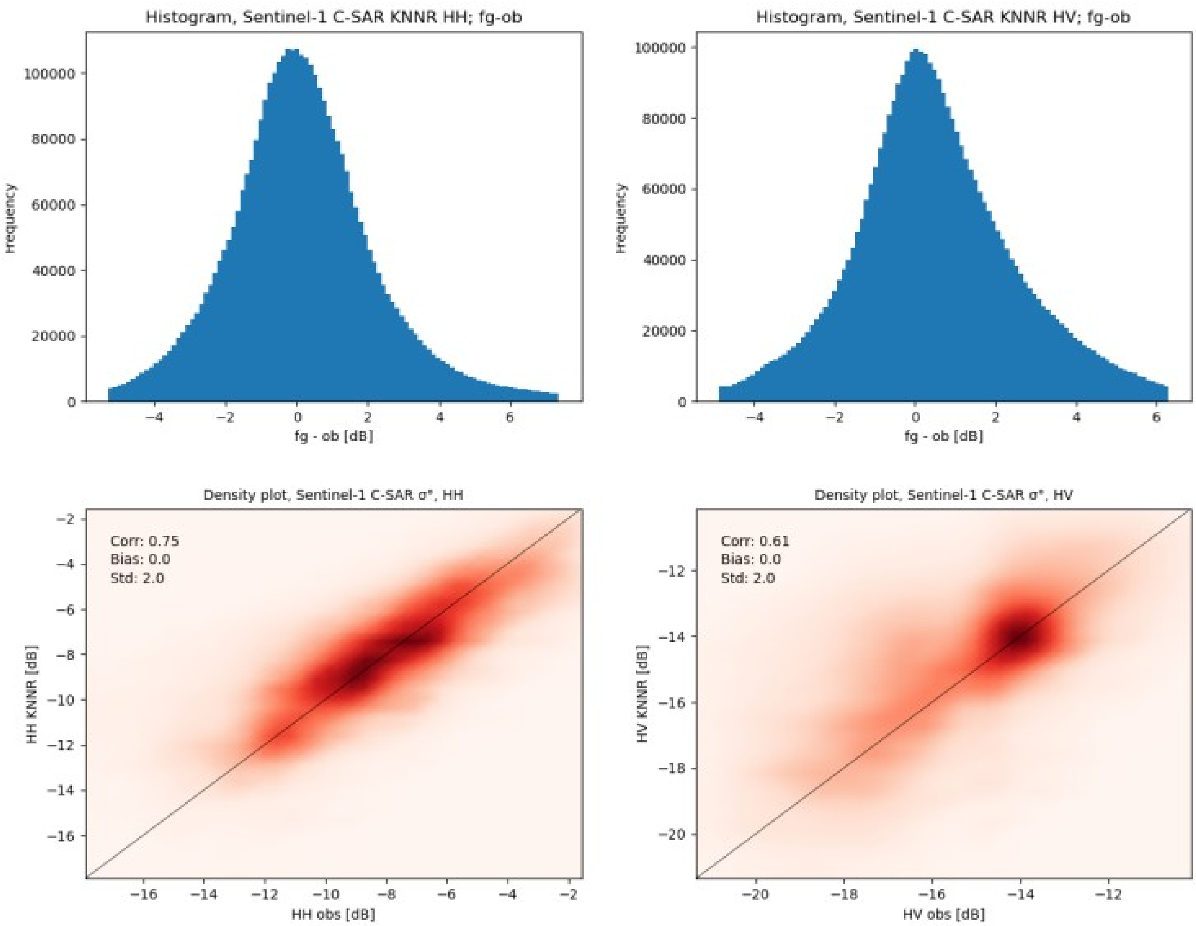

Figure 5. Upper row: Histogram for differences between KNNR modelled (fg) and observed (ob) radar backscatter from Sentinel-1 C-SAR. Bottom row: Scatterplots for observed and modelled backscatter. All data from Dec 2016 - may 2017. Left: HH polarization. Right: HV polarization.

The histogram for the differences between modelled and observed backscatter depicted in the top row of Figure 5 looks like a well behaved normal distribution which is the desired statistics for an entity to be assimilated. If the magnitude of the error is small enough to motivate assimilation is hard to tell. The sensor error is said to be -25 dB but the radiometric error is on the order of 1 dB (at three sigmas) which looks more promising. This is something that needs to be investigated in part 2 of this project.

Both the SMRT and KNNR models could be further improved by tuning. A sensitivity study was done to identify the most relevant input parameters, see section 3.4. Also tuning the models will be part of the next part of the project.

Table 6. Error statistics for Sentinel backscatter in case the fraction of ice is above 99 %.

RTM	Correlation	Bias	Std	RMSE
KNNR (HH / HV)	0.46 / 0.37	0.20 / 0.30	2.1 / 2.0	2.1 / 2.0
SMRT (HH / HV)	0.41 / 0.31	0.00 / 0.00	2.3 / 2.2	2.3 / 2.2

To find out which input parameters that contribute most to the prediction we calculated the Spearman correlation between the input variables and the KNNR output. While the standard Pearson's correlation assesses linear relationships, Spearman's correlation assesses monotonic relationships (whether linear or not). The correlations are presented in Table 7 (see Table 4 for an explanation of the abbreviations).

Table 6. Spearman correlation between different NEMO input parameters and measured Sentinel-1 C-SAR backscatter for the HH and HV polarizations. Correlations with a magnitude of 0.3 or greater are marked green.

	f_{ice}	h_{ice}	ts_{ice}	t_{ice}	s_{ice}	b_{ice}	h_{snw}	t_{snw}	u	v	s_{oce}	t_{oce}	sat_{az}	sat_{el}
HH	0.09	0.1	-0.06	-0.04	0.02	0.04	0.1	-0.08	0.09	-0.01	-0.07	-0.03	-0.01	0.77
HV	0.4	0.4	-0.31	-0.29	0.15	0.2	0.38	-0.35	0.03	0.05	-0.29	-0.32	0.01	0.51

The satellite elevation is very important when predicting the HH as well as the HV polarizations. For the HH polarization it is even the single input with a correlation above 0.1. For the HV polarization there are a number of other parameters that seem to be important. Here all parameters with the exception of the wind components and the satellite azimuth have a correlation above 0.1. Ice fraction, ice thickness, snow thickness, snow temperature and satellite elevation show a correlation with an absolute value at or above 0.4. A more detailed sensitivity analysis is presented in section 3.4.

3.3 Modelling AMSR2 brightness temperatures

For the open water there are a number of options available for modelling AMSR2 radiances. There is the CMEM model and also FASTEM, being part of the RTTOV package. We also tested with KNNR based on the positive experience from Sentinel. The result in terms of RMSE is shown in Table 8. Note that the CMEM output had to be transformed with a CDF matching technique in order to compensate for systematic deviations due to the absence of an atmosphere in the CMEM model. Also here the KNNR approach performed well.

Table 8. Error statistics in terms of RMSE for brightness temperatures [K] at AMSR2 points with only open water in its IFOV. Estimates from FASTEM simulations will be produced for the final report (TBA).

H/V	KNNR	CMEM (CDF)	FASTEM
ch 6.925	1.9 / 0.98	2.7 / 0.96	TBA
ch 7.3	2.2 / 1.1	3.0 / 1.0	TBA
ch 10.65	3.1 / 1.5	4.7 / 1.7	TBA
ch 18.7	10 / 5.3	16 / 8.3	TBA
ch 23.8	23 / 11	31 / 16	TBA
ch 36.5	15 / 6.6	20 / 8.5	TBA

For ice and snow surfaces the brightness temperatures for the different AMSR2 channels can be modelled with SMRT. The input from NEMO is identical to that used for modelling Sentinel-1C SAR with the exception that the satellite zenith angle is constant for AMSR2 being a conical scanning instrument. A separate comparison for ice is not possible for AMSR2 since there are two few cases where the AMSR2 IFOV has a large ice fraction. Instead we compared the results when using KNNR for the water part and SMRT for the ice/snow part with results from applying KNNR to all data, regardless of surface properties. The result of this comparison for all AMSR2 points is shown in Table 9. Again the SMRT output had to be CDF matched to avoid large systematic errors.

Table 9. Error statistics (H/V) for two different approaches for modelling AMSR2 brightness temperatures in different channels; combining KNNR for water and ice/snow (left) and using KNNR for water and SMRT for ice/snow (right). Note that there were too few points with ice within the IFOV to produce KNNR estimates for some of the AMSR channels (NA).

	KNNR (water) + KNNR (ice)		KNNR (water) + SMRT (ice/snow)	
H/V	Correlation	RMSE	Correlation	RMSE
ch 6.925	NA / NA	NA / NA	0.62 / 0.53	2.1 / 1.1
ch 7.3	NA / NA	NA / NA	0.62 / 0.46	2.3 / 1.2
ch 10.65	NA / NA	NA / NA	0.47 / 0.28	3.9 / 1.6
ch 18.7	NA / NA	NA / NA	0.36 / 0.25	8.2 / 4.3
ch 23.8	0.60 / 0.63	19 / 10	0.58 / 0.24	18 / 13
ch 36.5	0.58 / 0.59	10 / 8.5	0.61 / 0.17	15 / 9.6

The results are similar for the channels where there are enough cases with ice to make estimates based on KNNR. Again the KNNR method shows promising results. However, in order to be applicable we need to retrieve more cases where there is enough ice in the southern part of the domain to fill up the IFOV of the lower frequency AMSR2 channels.

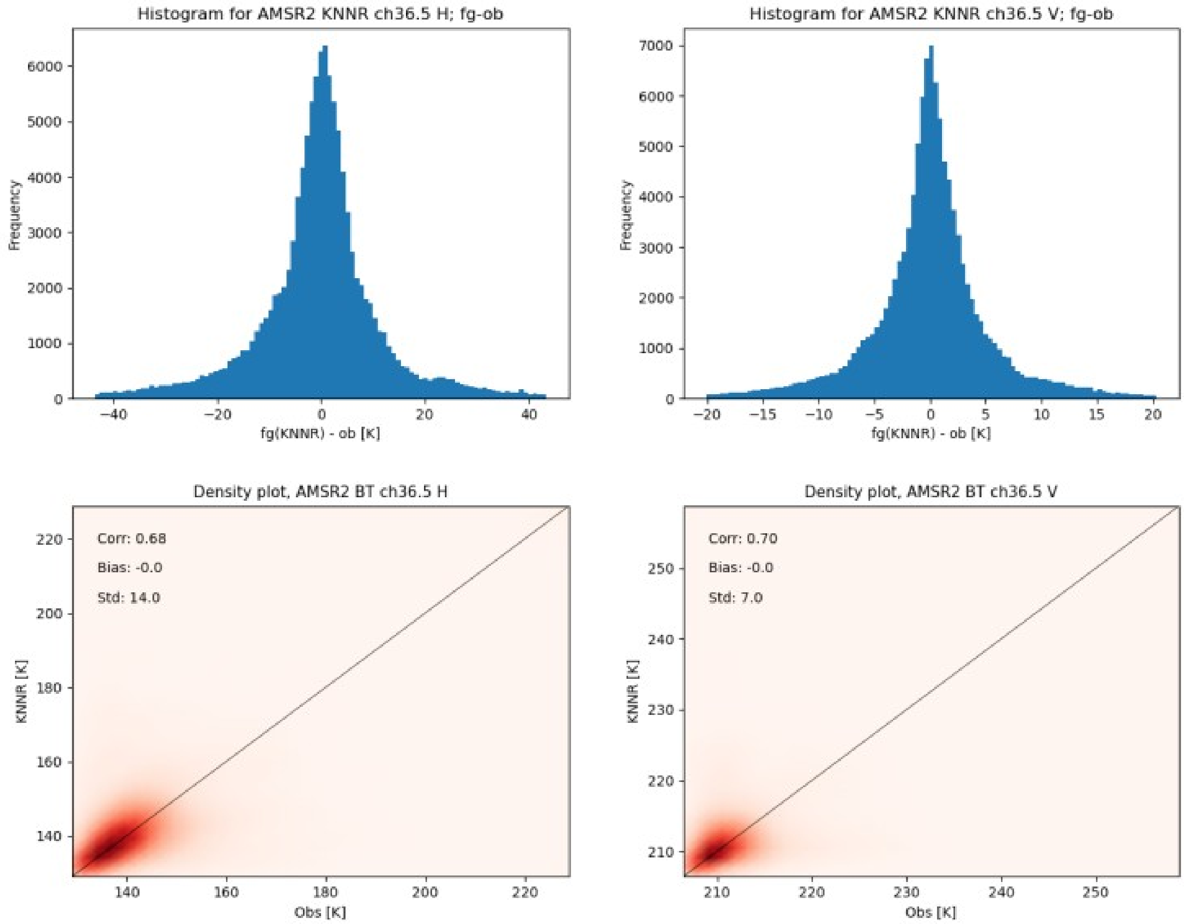

Figure 6. Example of error statistics for AMSR2 ch36.5. Top: Histogram for differences between KNNR modelled (fg) and observed (ob) brightness temperatures. Bottom: Scatterplots for the same observed and modelled brightness temperatures. All data relate to the period Dec 2016 - may 2017. Left: Horizontal polarization. Right: Vertical polarization.

In Figure 6 some error statistics are shown for the KNNR modelling of all AMSR2 points for the channel at 36.5 GHz. Corresponding figures for the other KNNR estimates of the AMSR2 channels (with ice within their IFOV) can be found in Appendix A7-A8, and maps for the sample date 2017-02-11 can be found in Appendix A9.

To find out which input parameters that contribute most to the AMSR2 predictions we again calculated the Spearman correlation between the input variables and the observed brightness temperatures. The correlations are presented in Table 10 (see Table 4 for an explanation of the abbreviations).

Table 10. Spearman correlation between different NEMO input parameters and measured AMSR2 brightness temperatures for the H and V polarizations of different channels. Correlations with a magnitude of 0.3 or greater are marked green.

H/V	ch 6.925	ch 7.3	ch 10.65	ch 18.7	ch 23.8	ch 36.5
f_{ice}	0.13 / -0.27	0.14 / -0.23	0.13 / -0.12	-0.02 / -0.09	0.04 / 0.03	0.19 / 0.12
h_{ice}	0.16 / -0.25	0.17 / -0.22	0.18 / -0.08	0.00 / -0.09	0.07 / 0.04	0.19 / 0.09
ts_{ice}	-0.07 / 0.25	-0..08 / 0.20	-0.06 / 0.20	0.29 / 0.42	0.25 / 0.30	-0.03 / 0.11
tm_{ice}	-0.09 / 0.20	-0.1 / 0.16	-0.08 / 0.15	0.25 / 0.36	0.25 / 0.30	-0.05 / 0.07
sm_{ice}	0.19 / -0.02	0.18 / 0.00	0.15 / -0.02	-0.02 / -0.11	-0.12 / -0.18	0.09 / -0.04
b_{ice}	0.16 / 0.00	0.14 / -0.01	0.12 / 0.02	0.18 / 0.15	0.14 / 0.12	0.16 / 0.07
h_{snw}	0.23 / -0.12	0.24 / -0.08	0.25 / -0.01	0.10 / -0.03	0.09 / 0.05	0.22 / 0.09
t_{snw}	-0.13 / 0.17	-0.15 / 0.12	-0.17 / 0.07	-0.01 / 0.10	-0.01 / 0.03	-0.18 /-0.05
u	0.31 / 0.12	0.30 / 0.14	0.25 / 0.07	0.23 / 0.11	0.16 / 0.10	0.09 / -0.09
v	0.19 / 0.18	0.18 / 0.19	0.21 / 0.24	0.32 / 0.35	0.31 / 0.32	0.27 / 0.28
$s_{wtr,opn}$	0.17 / -0.01	0.16 / 0.01	0.09 / 0.02	-0.01 / -0.05	-0.10 / -0.12	-0.09 / -0.13
$t_{wtr,opn}$	0.03 / 0.47	0.01 / 0.44	-0.01 / 0.24	0.14 / 0.13	0.05 / 0.03	-0.09 / -0.11
$s_{oce,ice}$	0.18 / -0.15	0.19 / -0.12	0.18 / -0.07	0.02 / -0.09	-0.11 / -0.16	0.09 / -0.03
$t_{oce,ice}$	-0.09 / -0.05	-0.11 / -0.10	-0.12 / -0.11	-0.07 / -0.08	-0.09 / -0.12	-0.04 / -0.16
sat_{az}	-0.01 / 0.08	-0.02 / 0.04	-0.04 / 0.06	-0.01 / 0.04	-0.02 / 0.00	-0.01 / 0.04

It is interesting to compare these findings to the channel specifications given in the figure by JAXA at https://suzaku.eorc.jaxa.jp/GCOM_W/w_amsr2/w_amsr2_wave.htm, here as Figure 7. From Table 9 we see that ch 6.9 (and 7.3) is sensitive to ice (and snow) temperature and thickness as well as wind speed and sea surface temperature (SST) which at least in parts correspond to the characteristics in Figure 7. The channel at 10.65 GHz shows correlations with wind speed and SST while the channels at 18.7 and 23.8 GHz correlate most with ice temperature and wind speed. Finally the channel at 36.5 GHz correlates with wind speed and to some extent also with snow depth.

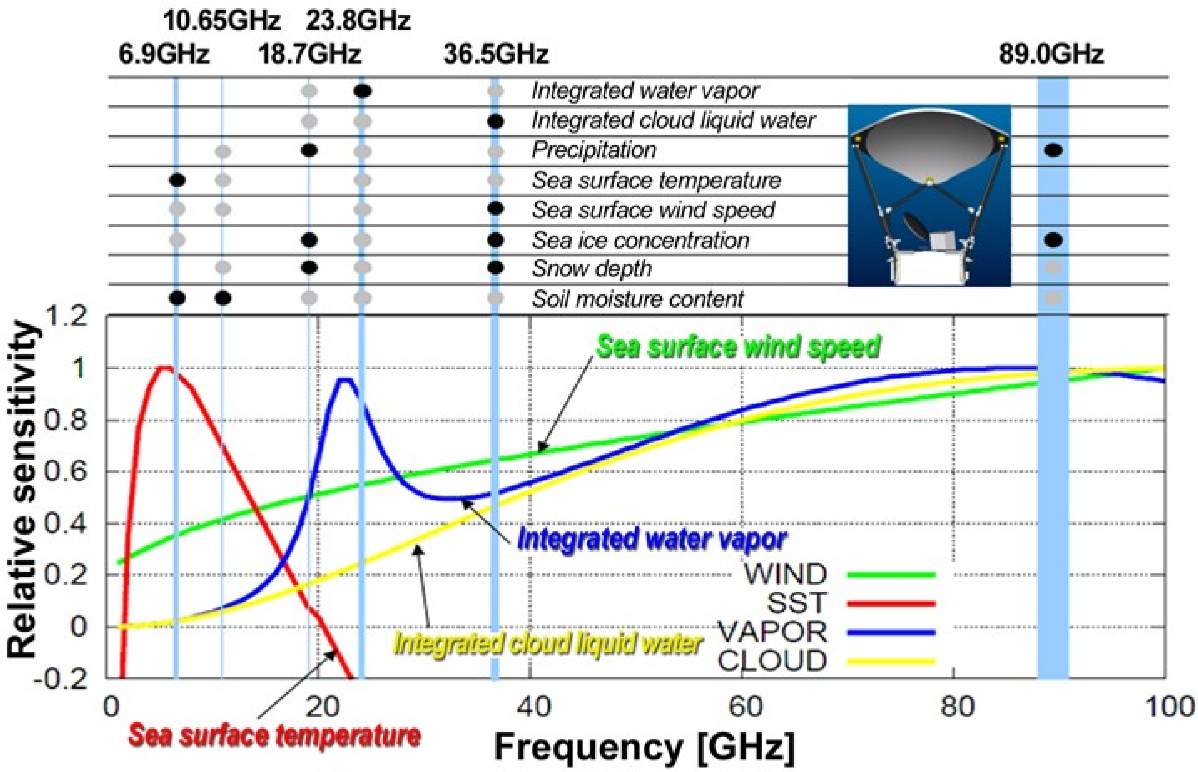

Figure 7. Schematic viewgraph of relative sensitivity to brightness temperature changes (normalized by maximum) for oceanic geophysical parameters. The original figure can be found at https://suzaku.eorc.jaxa.jp/GCOM_W/w_amsr2/w_amsr2_wave.html.

3.4 Sensitivity studies

To investigate the dependence of satellite radiances to surface properties modelled by the ice-ocean model, we decided it is best to use the physically-based SMRT model, rather than using the statistical KNNR model. We did this for both Sentinel-1 C-SAR data and for AMSR2 data, and all figures can be found in Appendix A1-A6. Explanations for all input variable names are given in Table 10, and a summary of all sensitivity experiments is given in Tables 11-13 below.

Table 11. Qualitative result regarding sensitivity of SMRT to ice type. “0” = not sensitive, “+” = sensitive, “0+” = slightly sensitive, “++” = very sensitive.

Variable or parameter	Sentinel 1C (HH/HV)	AMSR2 6.925 GHz (H/V)	AMSR2 7.300 GHz (H/V)	AMSR2 10.65 GHz (H/V)	AMSR2 18.7 GHz (H/V)	AMSR2 36.5 GHz (H/V)
ice type	++/+	++/++	++/++	++/++	++/++	++/++

Table 12. Qualitative result regarding sensitivity of SMRT to input variables. Reference ice type is set to "fresh" ice. "0" = not sensitive, "0+" = slightly sensitive, "+" = sensitive, "++" = very sensitive. "n/a" = "not applicable".

Variable or parameter	Sentinel-1 C-SAR (HH/HV)	AMSR2 6.925 GHz (H/V)	AMSR2 7.300 GHz (H/V)	AMSR2 10.65 GHz (H/V)	AMSR2 18.7 GHz (H/V)	AMSR2 36.5 GHz (H/V)
h_{snw}	+/0	0+/0+	0+/0+	0+/0+	0+/0+	0+/0+
t_{snw}	0/0	0/0	0/0	0/0	0/0	0/0
d_{snw}	0/0	0+/0	0+/0	0+/0	0+/0	0+/0
l_{snw}	0/+	0/0	0/0	0/0	0/0	0/0
h_{ice}	+/+	+/+	+/+	+/+	+/+	+/+
t_{ice}	0/0	0/0	0/0	0/0	0/0	0/0
s_{ice}	n/a	n/a	n/a	n/a	n/a	n/a
r_{ice}	+/+	0/0	0/0	0+/0+	+/+	+/+
p_{ice}	0/0	++/++	++/++	++/++	+/+	0+/0+
t_{oce}	0/0	0/0	0/0	0/0	0/0	0/0
s_{oce}	0/0	0/0	0/0	0/0	0/0	0/0

Table 13. Qualitative result regarding sensitivity of SMRT to input variables. Reference ice type is set to "first-year" ice. "0" = not sensitive, "0+" = slightly sensitive, "+" = sensitive, "++" = very sensitive.

Variable or parameter	Sentinel-1 C-SAR (HH/HV)	AMSR2 6.925 GHz (H/V)	AMSR2 7.300 GHz (H/V)	AMSR2 10.65 GHz (H/V)	AMSR2 18.7 GHz (H/V)	AMSR2 36.5 GHz (H/V)
h_{snw}	+/0	0/0	0/0	0/0	0/0	0+/0
t_{snw}	0/0	0/0	0/0	0/0	0/0	0/0
d_{snw}	0/+	0+/0	0+/0	0+/0	0+/0	0+/0+
l_{snw}	+/+	0/0	0/0	0/0	0/0	0/0
h_{ice}	+/+	0+/0+	0+/0+	0+/0+	0/0	0/0
t_{ice}	+/+	+/+	+/+	+/+	+/+	+/+
s_{ice}	+/+	+/+	+/+	+/+	+/+	+/+
r_{ice}	+/+	0/0	0/0	0/0	0/0	0+/0+
p_{ice}	0/0	0/0	0/0	0/0	0/0	0/0
t_{oce}	0/0	0/0	0/0	0/0	0/0	0/0
s_{oce}	0/0	0/0	0/0	0/0	0/0	0/0

4. Discussion and Future Outlook

The goal of this project was to start studying how to use satellite data (Sentinel-1 C-band synthetic aperture radar data and AMSR2 passive microwave data, both of which are rather insensitive to the state of the atmosphere) together with Radiative Transfer Models to compute NEMO model equivalents. We have evaluated a number of RTM combinations and found that the statistical (machine learning) method known as k nearest neighbour regression performed best. The idea is then to use these model equivalents to constrain the initial state of the NEMO ice-ocean model by means of a data assimilation method. Whether or not the quality of these model equivalents (and the NEMO model itself) is sufficient to help in doing so is a question to be answered in the next project phase. Even if it is known that NEMO today often has too much ice (as in Figure 3), starting out by assimilating satellite information before the onset of the ice season may very well improve the situation. Although the KNNR method turned out to be competitive it does not mean that the other RTM models should be ruled out. There are many parameters to tune and it may be possible to come up with a setup that matches the performance of the KNNR method. However, also the KNNR method has some parameters that could be tuned.

Another improvement could be to replace the KNNR with other ML structures, e.g. a multi layer perceptron. Such a structure would have the ability to fit even better to the data. So far we haven't bothered much with quality control of the satellite data. We noted that the Sentinel data sometimes has thermal noise in parts of the image. This should be mitigated and other quality information be included in the processing (like data quality flags).

The higher frequency channels of AMSR2 are more sensitive to the atmospheric state than the ones at 6.9, 7.3 and 10.7 Ghz. In order to improve the accuracy when modelling these higher frequencies one has to take the atmosphere into consideration. This could be done using the RTTOV model together with information from a numerical weather prediction (NWP) model.

To simplify things when modelling the AMSR2 IFOV we assumed it to be circular and proceeded to calculate the model equivalents based on two weighted NEMO states for the open ocean and ice/snow parts respectively. This should be fine as long as the RTM is not too non-linear. This has however not been confirmed. One should compare the current strategy to what one gets if computing AMSR2 data for each NEMO grid point separately and then average them according to the IFOV. This method is more correct, but also much more time consuming.

In order to have better coverage for the AMSR2 data the contributions from land surfaces in coastal areas need to be taken into consideration. Again such information is available from the NWP system. This is one of the challenges to be tackled in the related project "Consistent Air-Ice-Sea Data Assimilation of Satellite Observations (CAISA)" that has now been funded by the Swedish National Space Board.

References

Axell, L.B. and Y. Liu, 2016. Application of 3-D ensemble variational data assimilation to a Baltic Sea reanalysis 1989-2013, Tellus A 2016, 68, 24220, http://dx.doi.org/10.3402/tellusa.v68.24220.

Axell, L. and Y. Liu, 2017. Ensemble-based data assimilation of observations into NEMO-Nordic, Proceedings of the Eighth EuroGOOS International Conference, Bergen, 3-5 October 2017.

Hordoir, R., Axell, L., Höglund, A., Dieterich, C., Fransner, F., Gröger, M., Liu, Y., Pemberton, P., Schimanke, S., Andersson, H., Ljungemyr, P., Nygren, P., Falahat, S., Nord, A., Jönsson, A., Lake, I., Döös, K., Hieronymus, M., Dietze, H., Löptien, U., Kuznetsov, I., Westerlund, A., Tuomi, L., Haapala, J., 2019. Nemo-nordic 1.0: a nemo-based ocean model for the Baltic and North seas - research and operational applications. Geosci. Model Dev. 12, 363–386. https://doi.org/10.5194/gmd-12-363-2019.

Kudryavtsev, V., Akimov, D., Johannessen, J. A., & Chapron, B. (2005). On radar imaging of current features: 1. Model and comparison with observations. Journal of Geophysical Research, 110, C07016. https://doi.org/10.1029/2004JC002505

Panofsky, H. W. and Brier, G. W.: Some Applications of Statistics to Meteorology, The Pennsylvania State University Press, Philadelphia, 1968.

Pedregosa, F., Varoquaux, Ga"el, Gramfort, A., Michel, V., Thirion, B., Grisel, O., … others. (2011). Scikit-learn: Machine learning in Python. Journal of Machine Learning Research, 12(Oct), 2825–2830.

Pemberton, P., Löptien, U., Hordoir, R., Höglund, A., Schimanke, S., Axell, L., Haapala, J., 2017. Sea-ice evaluation of NEMO-Nordic 1.0: a NEMO–LIM3.6-based ocean–sea-ice model setup for the North Sea and Baltic Sea. Geosci. Model Dev. 10, 3105–3123. https://doi.org/10.5194/gmd-10-3105-2017.

Picard, G., Sandells, M., and Löwe, H.: SMRT: an active–passive microwave radiative transfer model for snow with multiple microstructure and scattering formulations (v1.0), Geosci. Model Dev., 11, 2763–2788, https://doi.org/10.5194/gmd-11-2763-2018, 2018.

Romeiser, R., and D.R. Thompson, Numerical study on the along-track interferometric radar imaging mechanism of oceanic surface currents, IEEE Trans. on Geosci. and Remote Sensing, 38-II, 446-458, 2000.

de Rosnay, P., Muñoz-Sabater, J., Albergel, C., Isaksen, L., English, L., Drusch, M., Wigneron, J-P. SMOS brightness temperature forward modelling and long term monitoring at ECMWF, Remote Sensing of Environment, Volume 237, 111424, https://doi.org/10.1016/j.rse.2019.111424.

Saunders, R. , Hocking, J., Turner, E., Havemann, S., , Geer, A., Lupu, C., Vidot, J., Chambon, P., Köpken-Watts, C., Scheck, L., Stiller, O., Stumpf, C., Borbas, E. RTTOV-13 SCIENCE AND VALIDATION REPORT, accessed 10 May 2021: http://nwp-saf.eumetsat.int/site/download/documentation/rtm/docs_rttov13/rttov13_svr.pdf

Appendix

A1. Sensitivity studies: SMRT with Sentinel-1 C-band data

Sensitivity to h_{snw}

Ice type: “fresh ice”

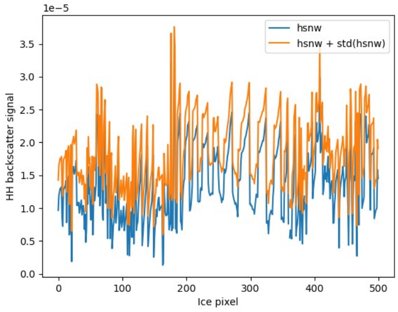

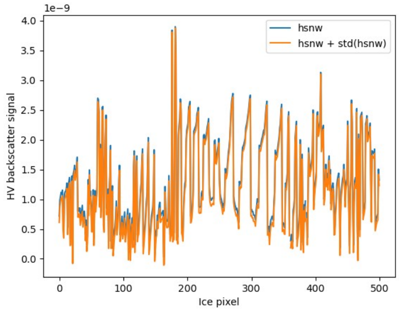

Ice type: “first-year ice”

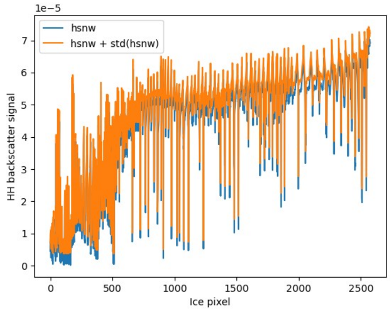

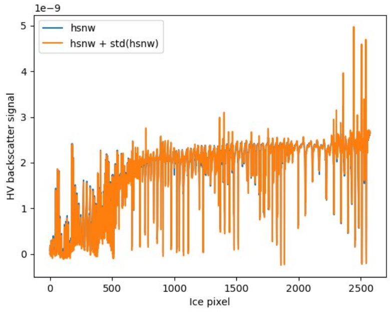

Sensitivity to t_{snw}

Ice type: “fresh ice”

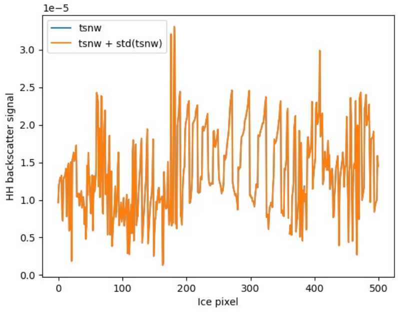

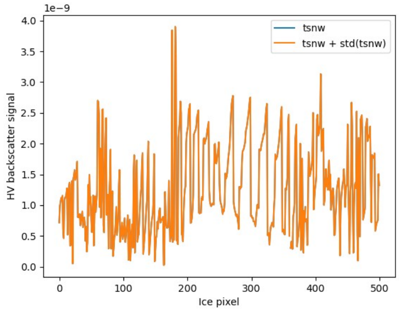

Ice type: “first-year ice”

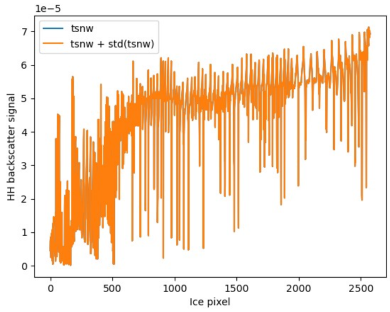

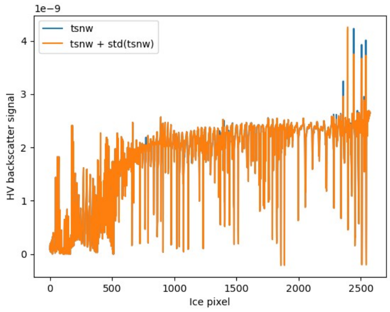

Sensitivity to d_{snw}

Ice type: “fresh ice”

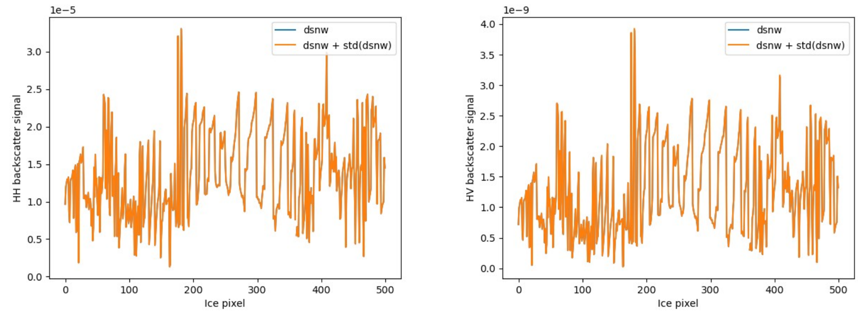

Ice type: “first-year ice”

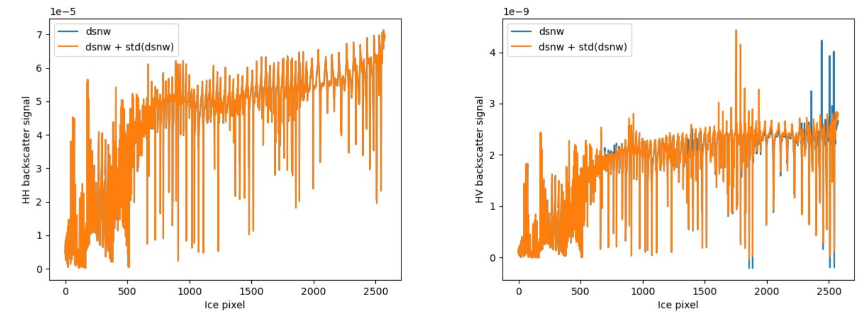

Sensitivity to l_{snw}

Ice type: “fresh ice”

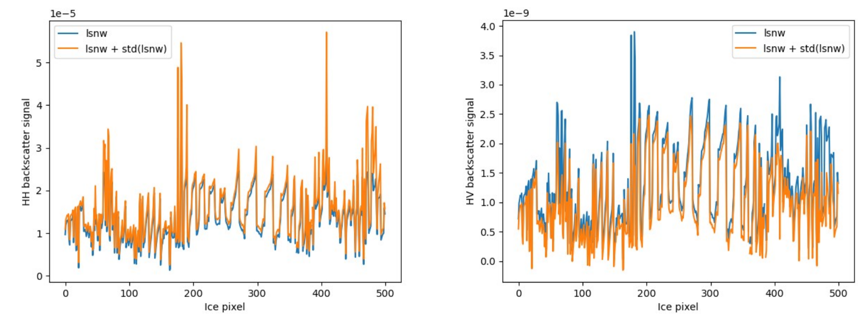

Ice type: “first-year ice”

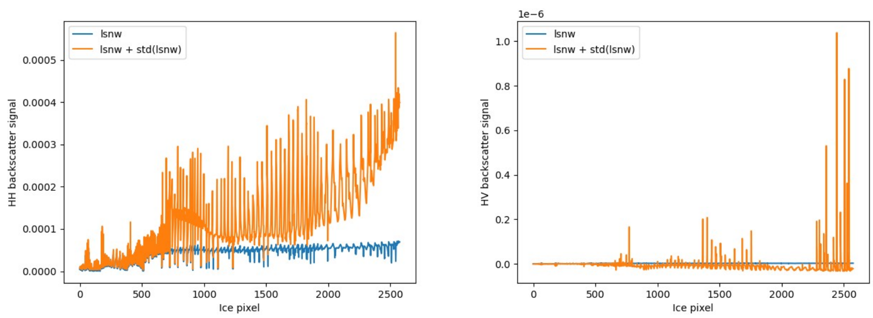

Sensitivity to h_{ice}

Ice type: “fresh ice”

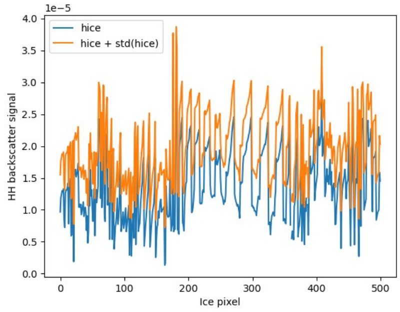

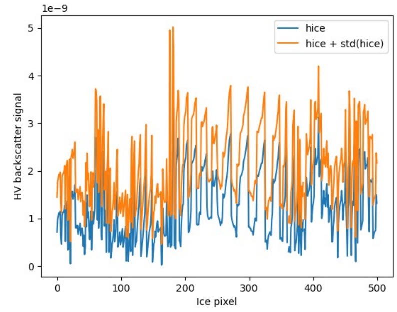

Ice type: “first-year ice”

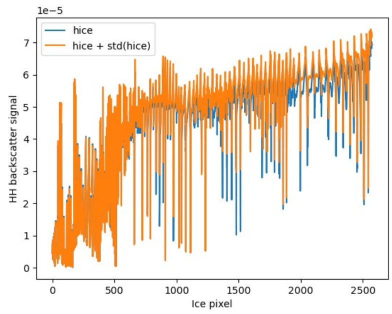

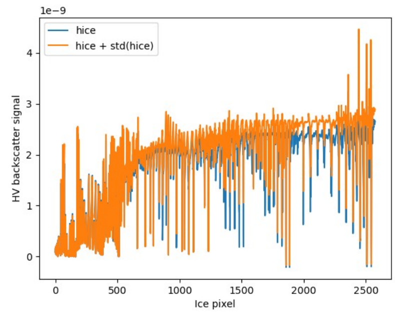

Sensitivity to t_{ice}

Ice type: “fresh ice”

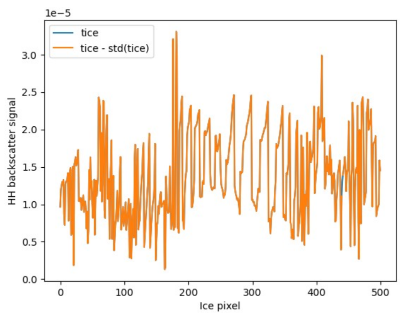

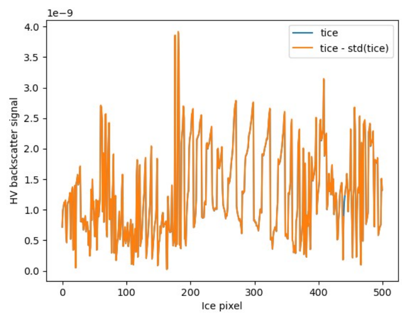

Ice type: “first-year ice”

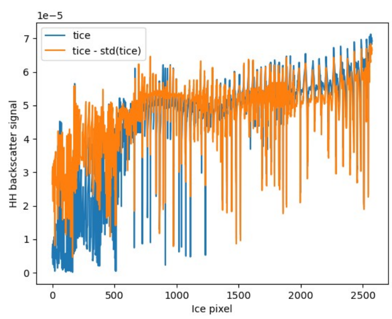

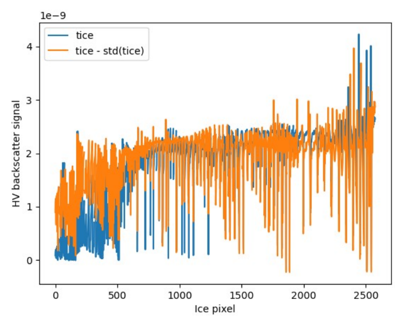

Sensitivity to s_{ice}

Ice type: “fresh ice”

(not applicable) (not applicable)

Ice type: “first-year ice”

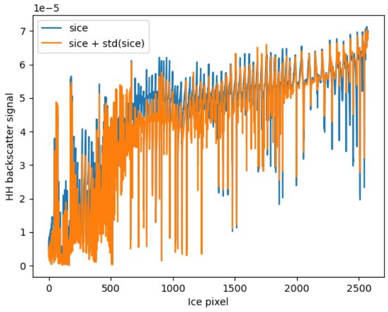

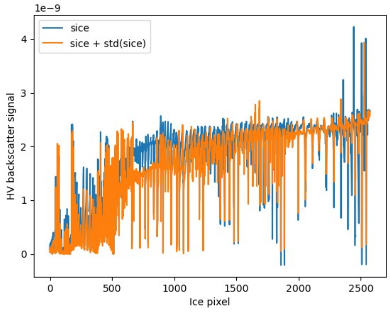

Sensitivity to r_{ice}

Ice type: “fresh ice”

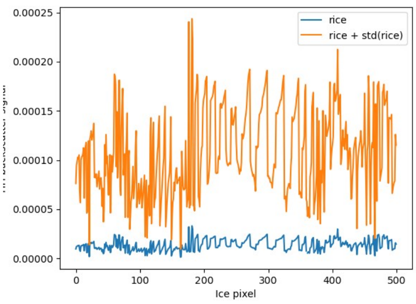

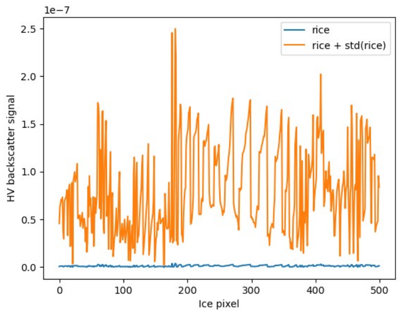

Ice type: “first-year ice”

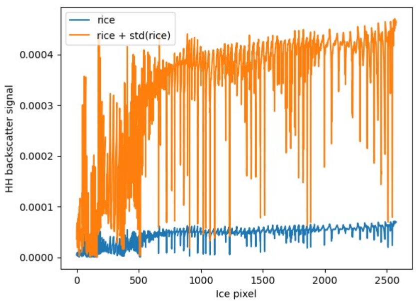

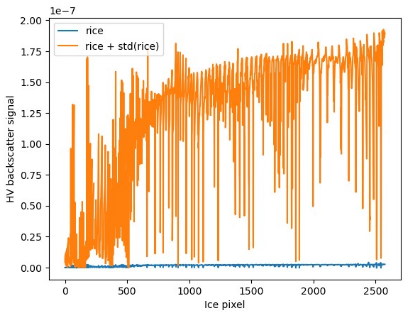

Sensitivity to p_{ice}

Ice type: “fresh ice”

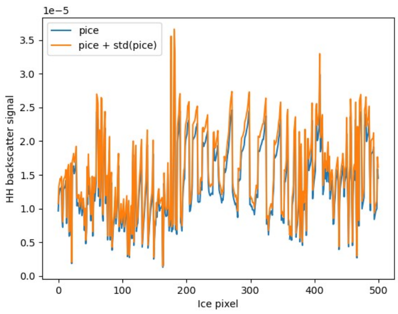

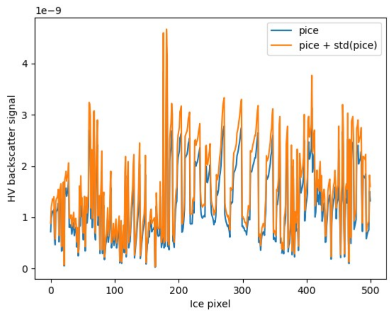

Ice type: “first-year ice”

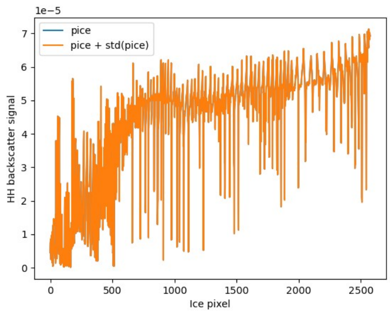

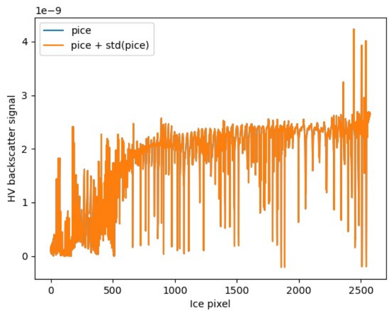

Sensitivity to ice type

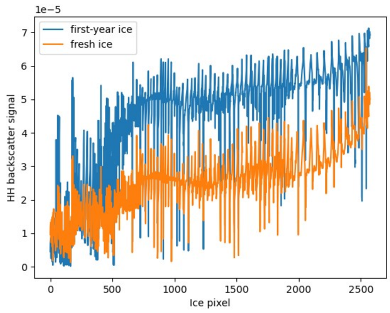

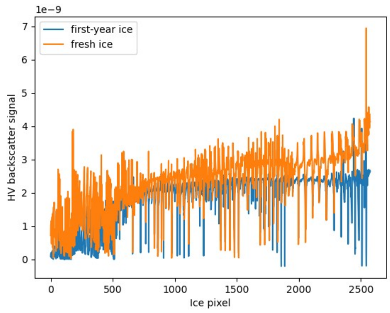

Sensitivity to t_{oce}

Ice type: “fresh ice”

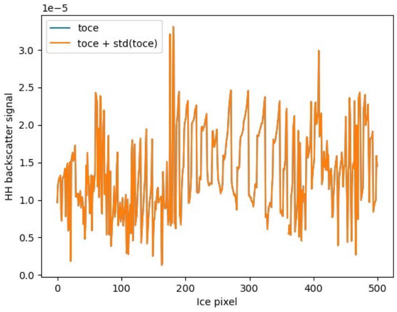

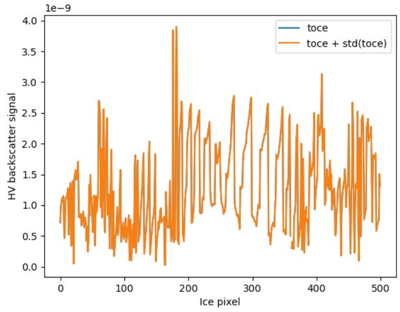

Ice type: “first-year ice”

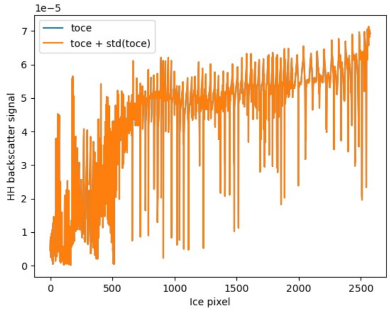

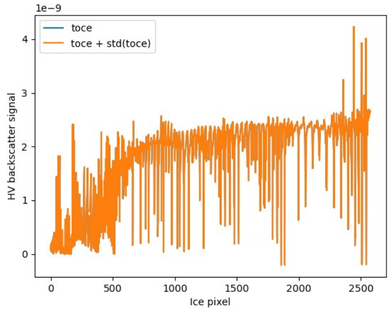

Sensitivity to s_{oce}

Ice type: “fresh ice”

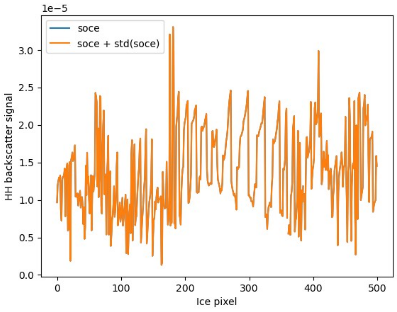

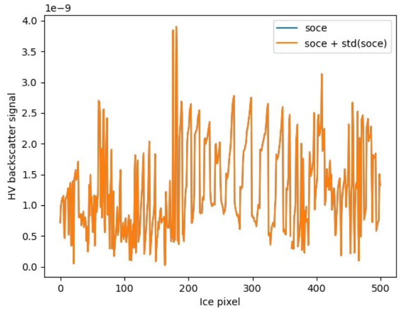

Ice type: “first-year ice”

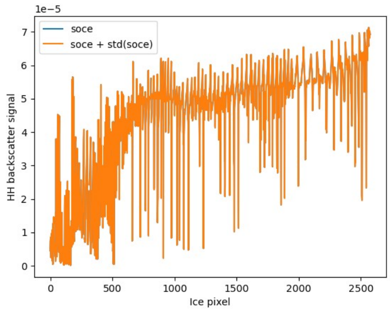

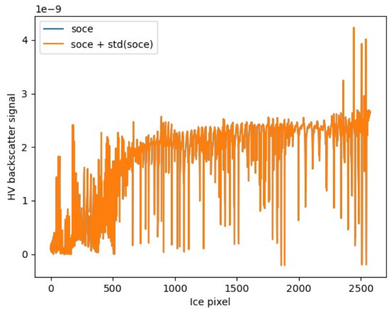

A2. Sensitivity studies: SMRT with AMSR2 6.925 GHz data

Sensitivity to h_{snw}

Ice type: “fresh ice”

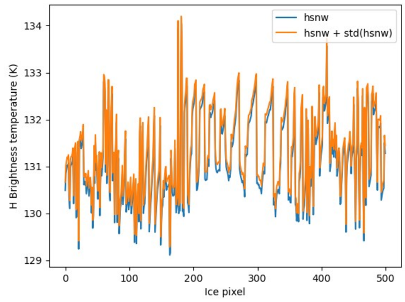

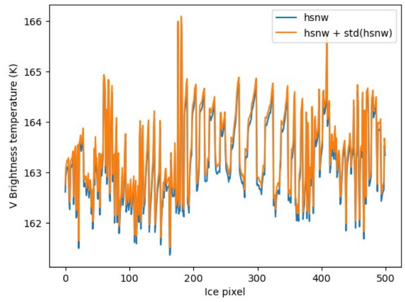

Ice type: “first-year ice”

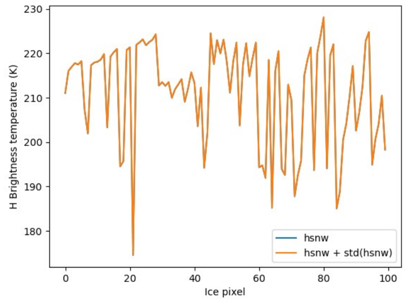

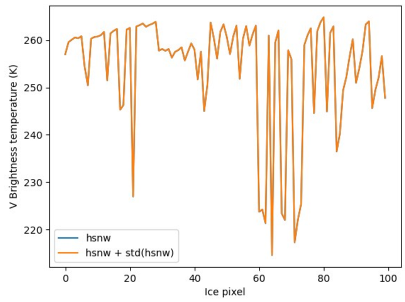

Sensitivity to t_{snw}

Ice type: “fresh ice”

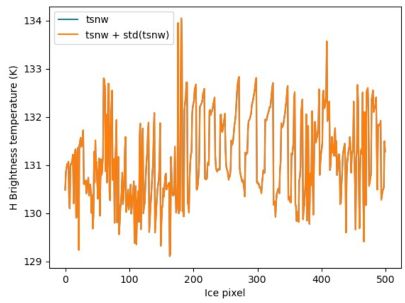

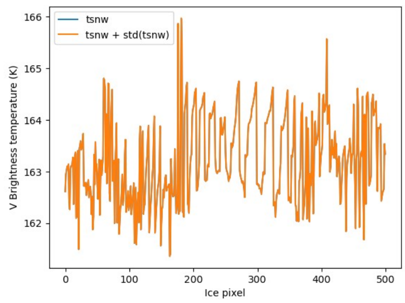

Ice type: “first-year ice”

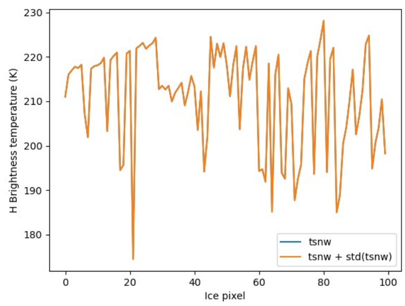

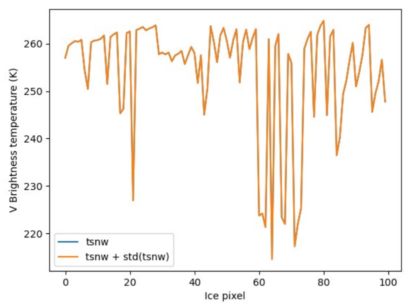

Sensitivity to d_{snw}

Ice type: “fresh ice”

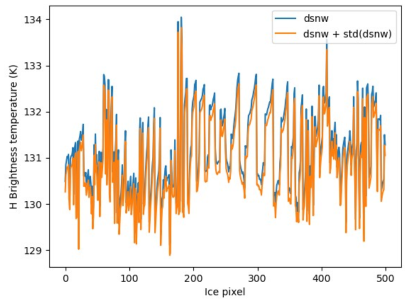

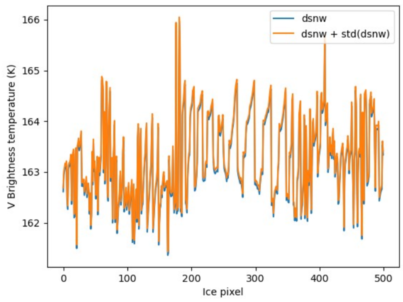

Ice type: “first-year ice”

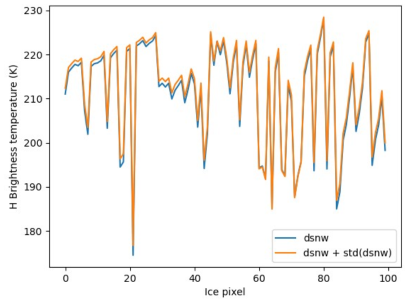

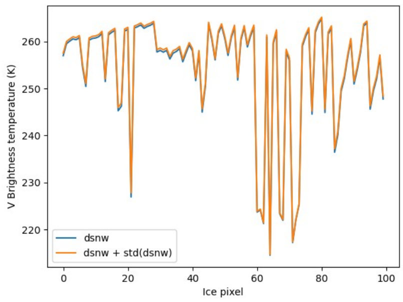

Sensitivity to l_{snw}

Ice type: “fresh ice”

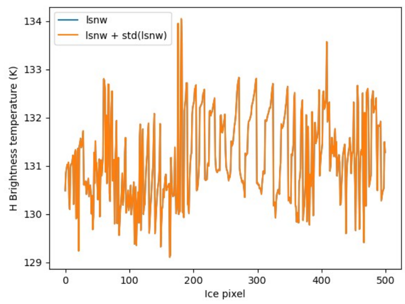

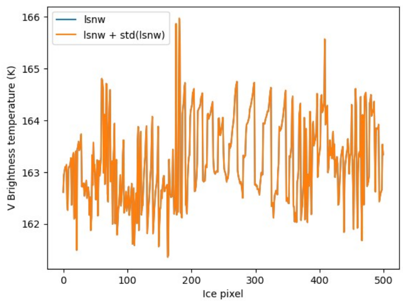

Ice type: “first-year ice”

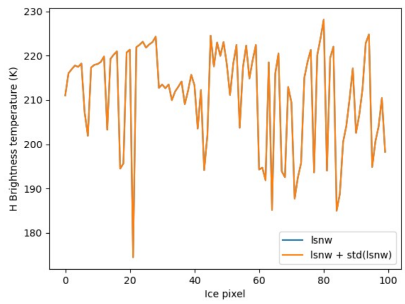

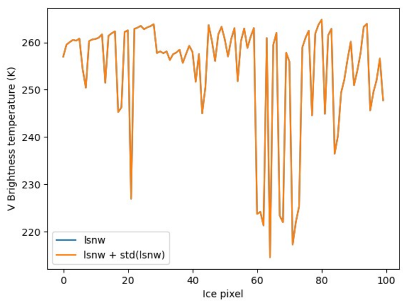

Sensitivity to h_{ice}

Ice type: “fresh ice”

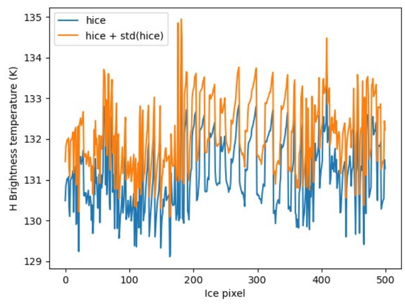

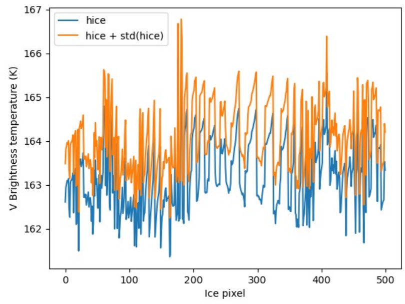

Ice type: “first-year ice”

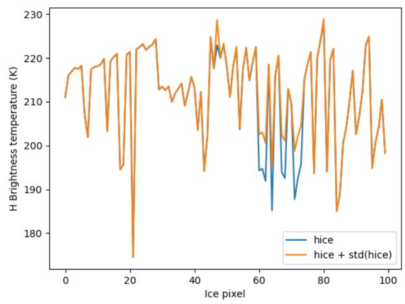

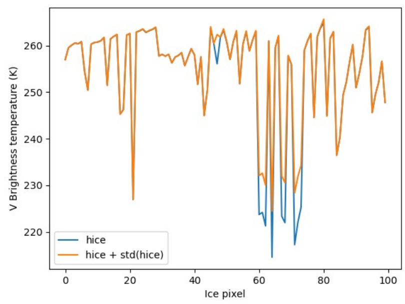

Sensitivity to t_{ice}

Ice type: “fresh ice”

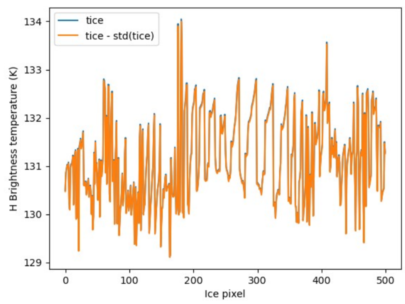

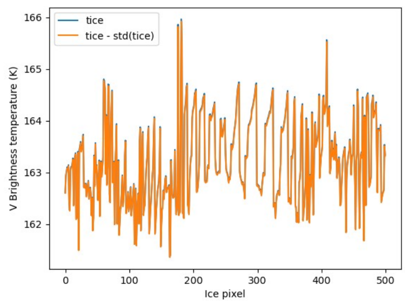

Ice type: “first-year ice”

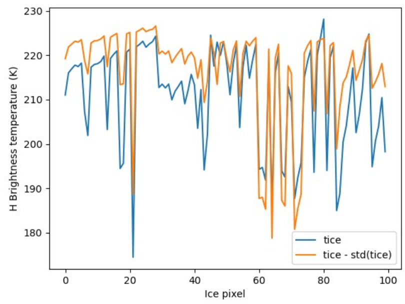

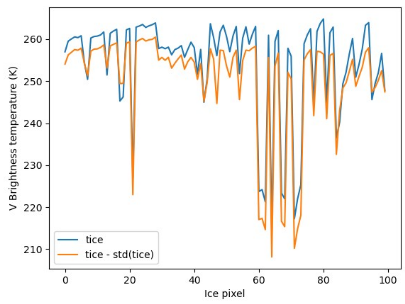

Sensitivity to s_{ice}

Ice type: “fresh ice”

(not applicable) (not applicable)

Ice type: “first-year ice”

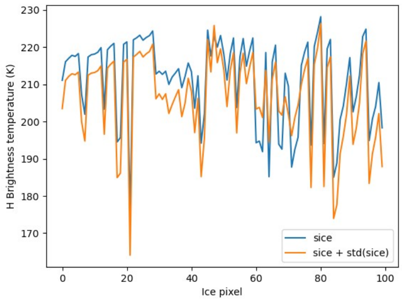

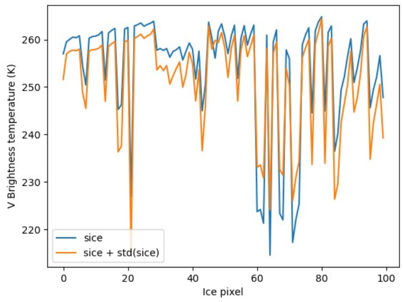

Sensitivity to r_{ice}

Ice type: “fresh ice”

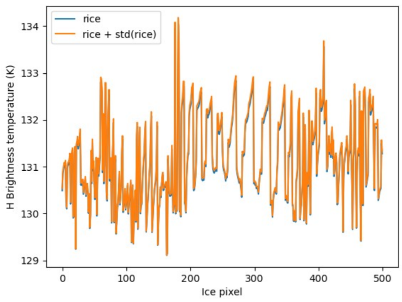

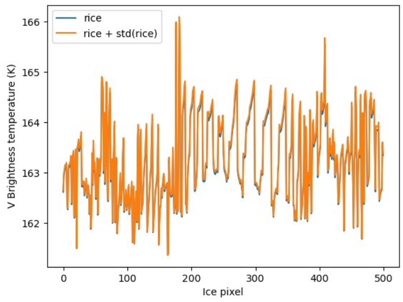

Ice type: “first-year ice”

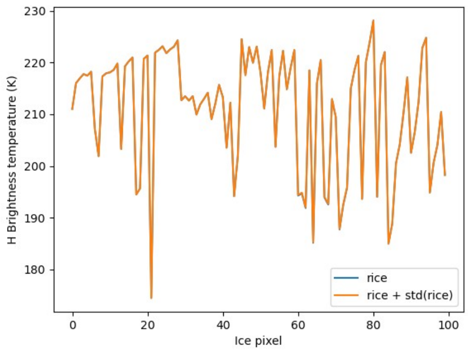

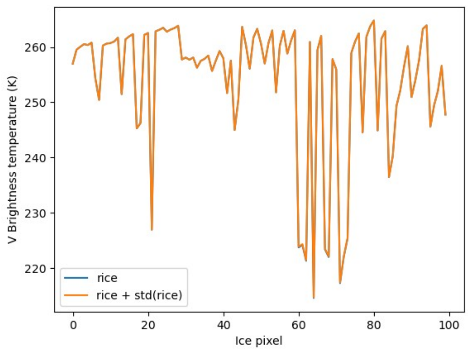

Sensitivity to p_{ice}

Ice type: “fresh ice”

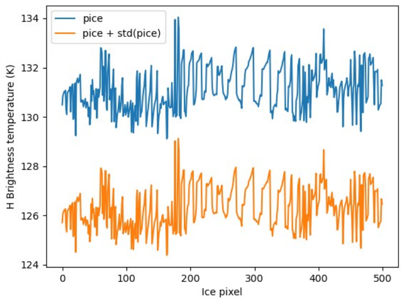

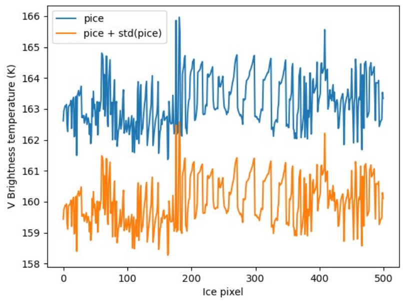

Ice type: “first-year ice”

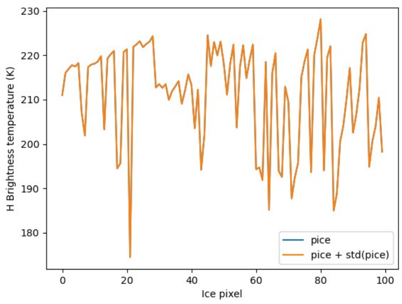

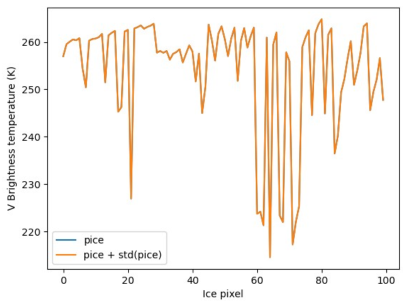

Sensitivity to ice type

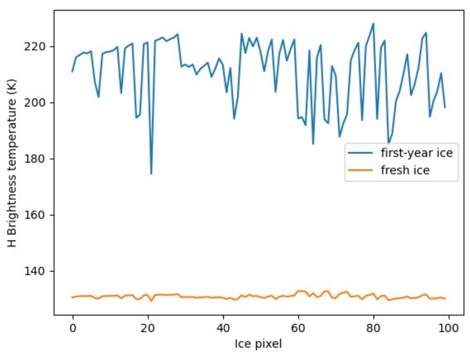

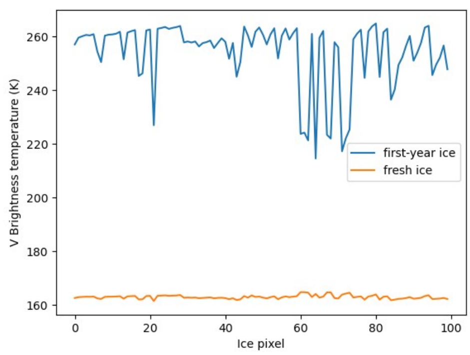

Sensitivity to t_{oce}

Ice type: “fresh ice”

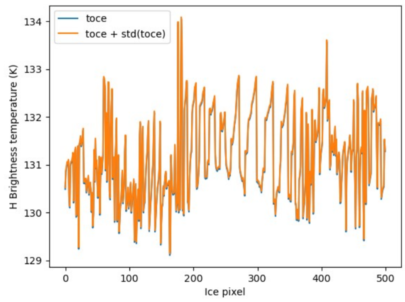

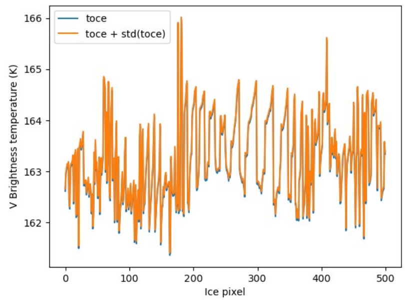

Ice type: “first-year ice”

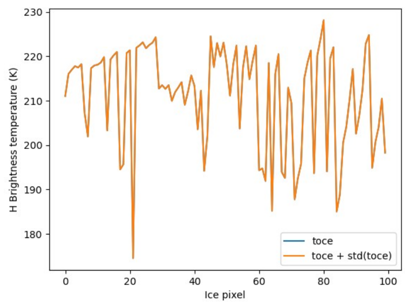

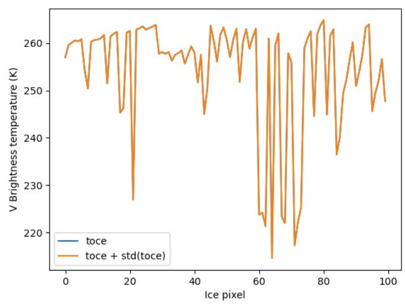

Sensitivity to s_{oce}

Ice type: “fresh ice”

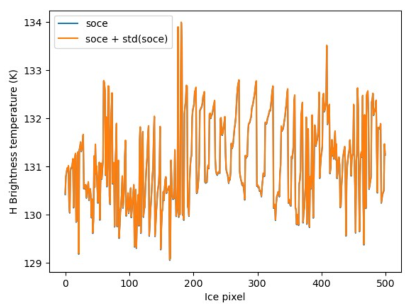

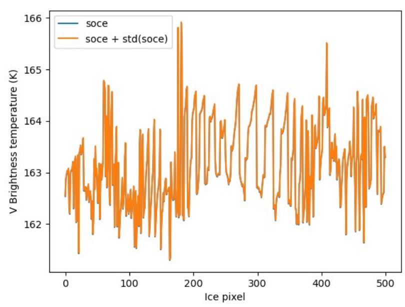

Ice type: “first-year ice”

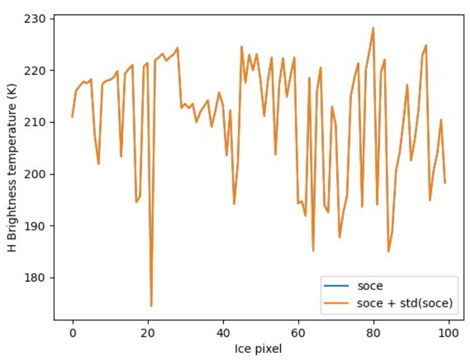

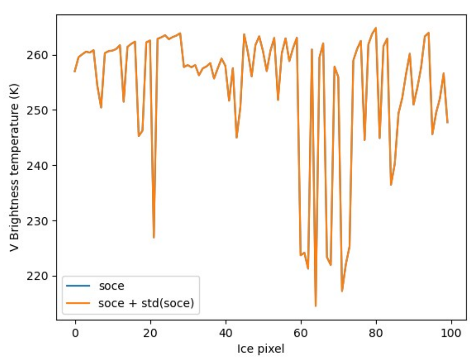

A3. Sensitivity studies: SMRT with AMSR2 7.3 GHz data

Sensitivity to h_{snw}

Ice type: “fresh ice”

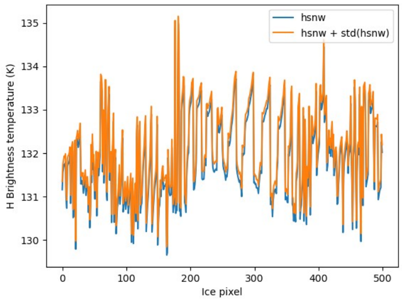

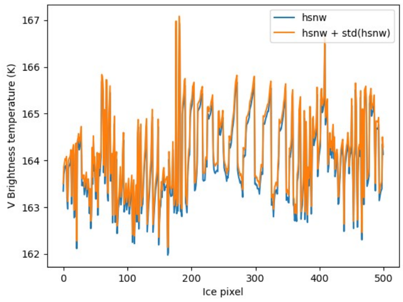

Ice type: “first-year ice”

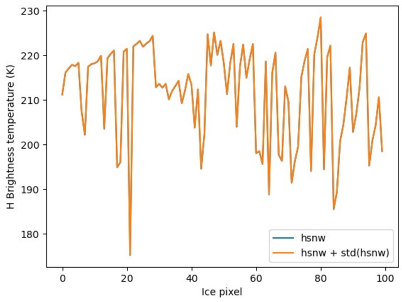

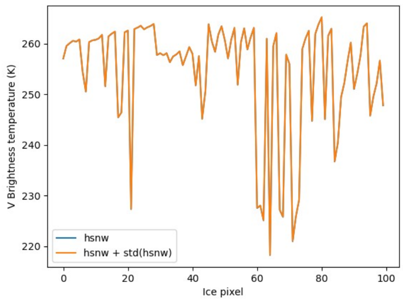

Sensitivity to t_{snw}

Ice type: “fresh ice”

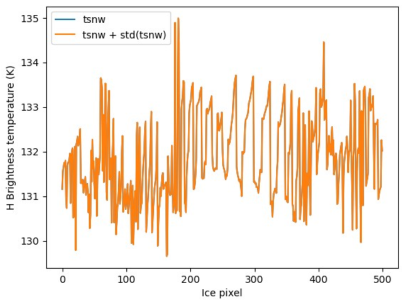

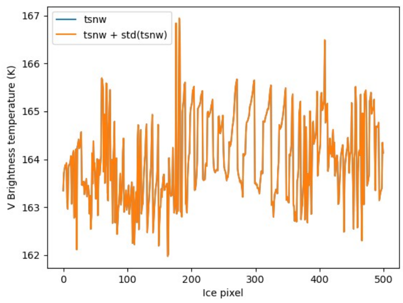

Ice type: “first-year ice”

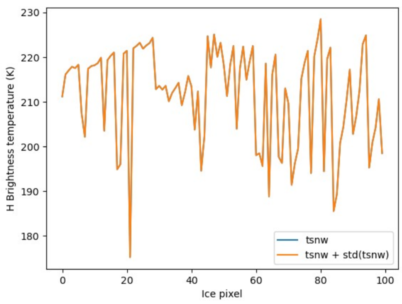

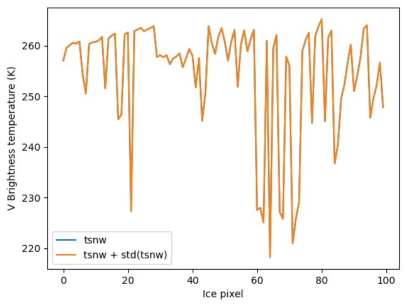

Sensitivity to d_{snw}

Ice type: “fresh ice”

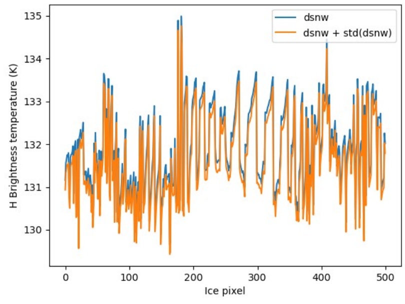

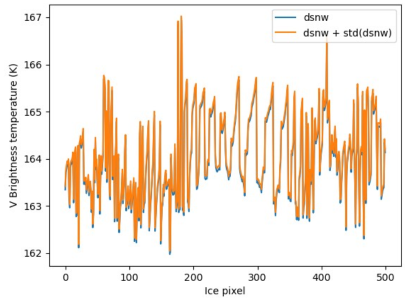

Ice type: “first-year ice”

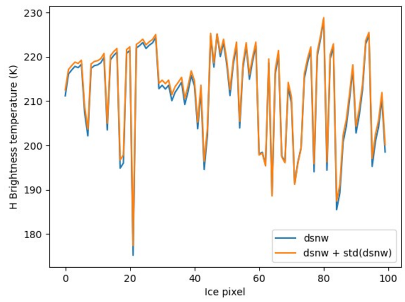

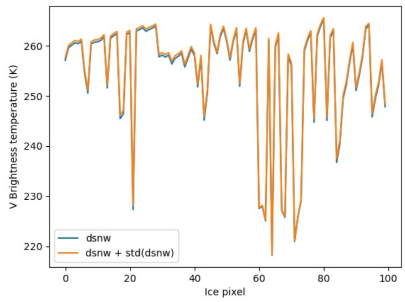

Sensitivity to l_{snw}

Ice type: “fresh ice”

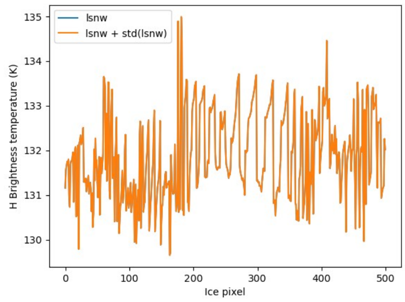

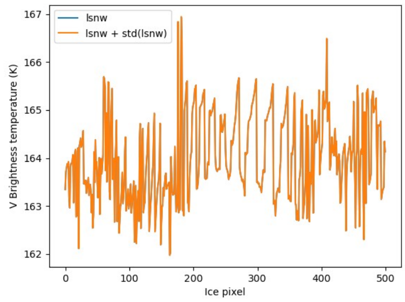

Ice type: “first-year ice”

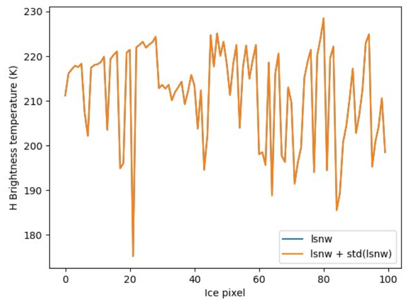

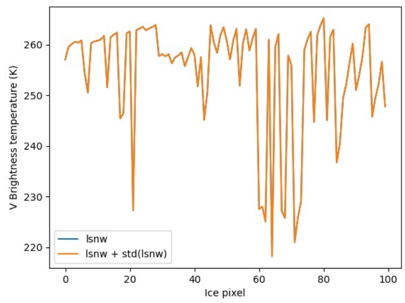

Sensitivity to *h_{ice}*

Ice type: “fresh ice”

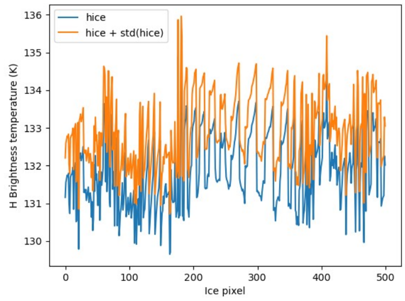

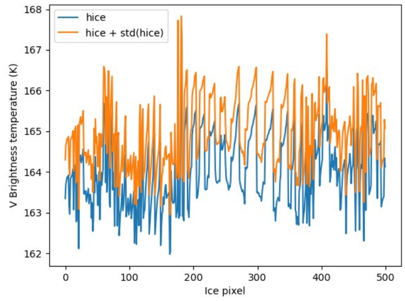

Ice type: “first-year ice”

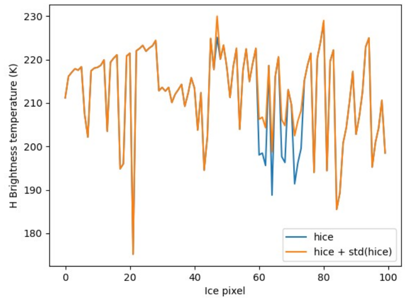

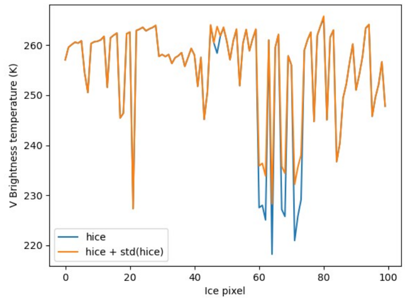

Sensitivity to *t_{ice}*

Ice type: “fresh ice”

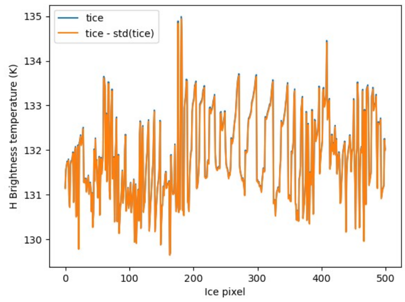

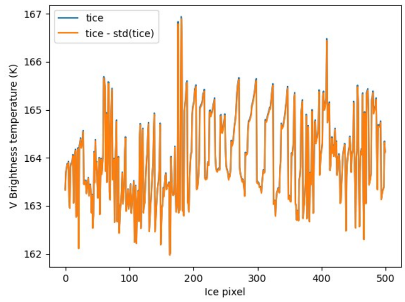

Ice type: “first-year ice”

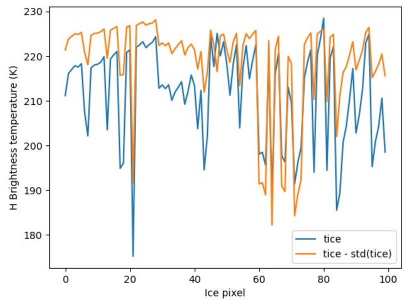

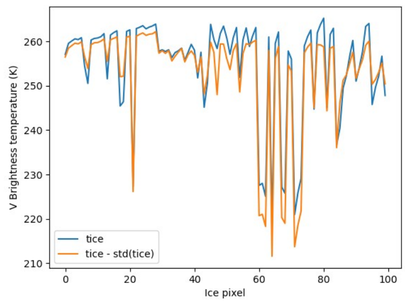

Sensitivity to s_{ice}

Ice type: “fresh ice”

(not applicable) (not applicable)

Ice type: “first-year ice”

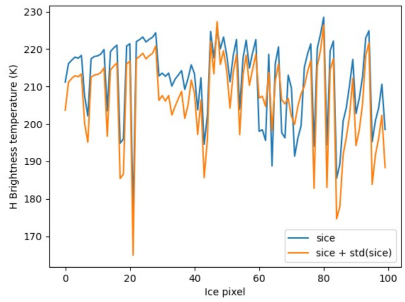

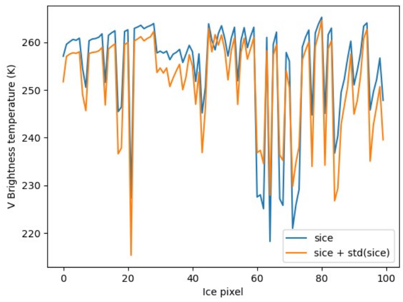

Sensitivity to r_{ice}

Ice type: “fresh ice”

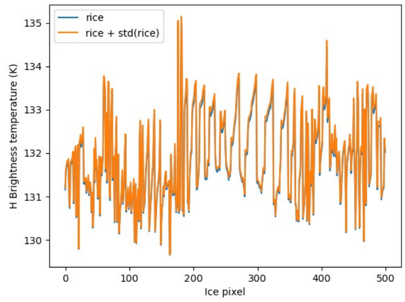

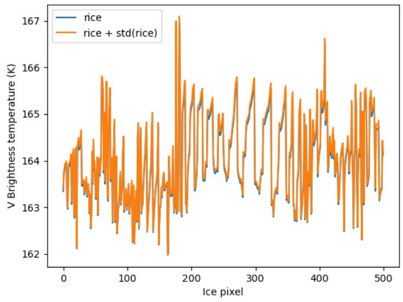

Ice type: “first-year ice”

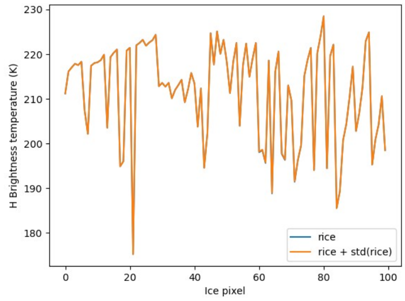

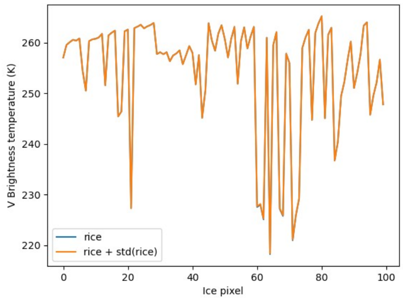

Sensitivity to p_{ice}

Ice type: “fresh ice”

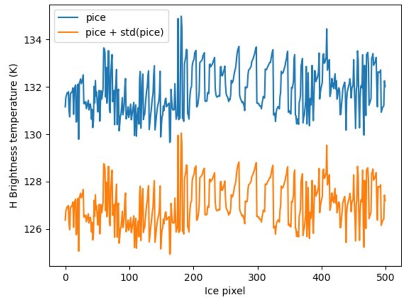

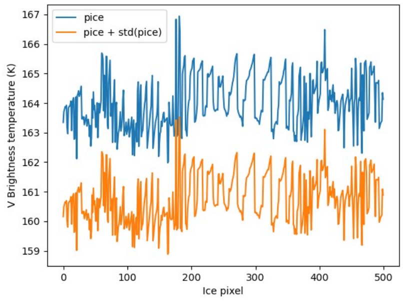

Ice type: “first-year ice”

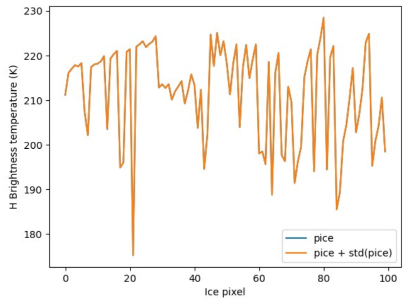

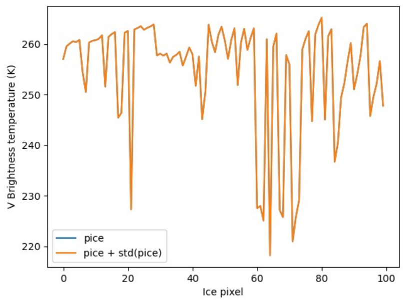

Sensitivity to ice type

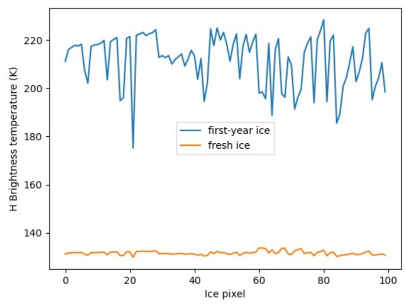

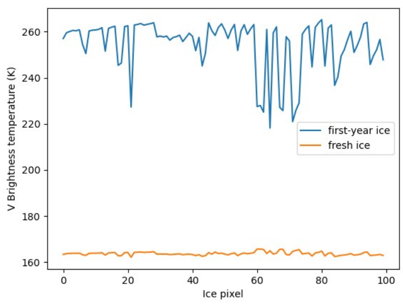

Sensitivity to t_{oce}

Ice type: “fresh ice”

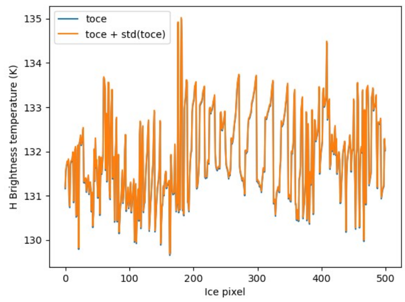

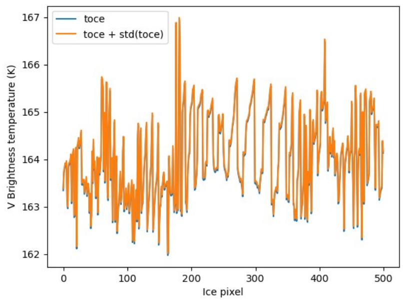

Ice type: “first-year ice”

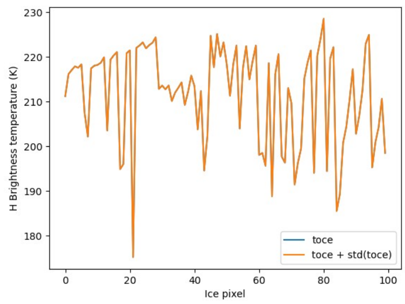

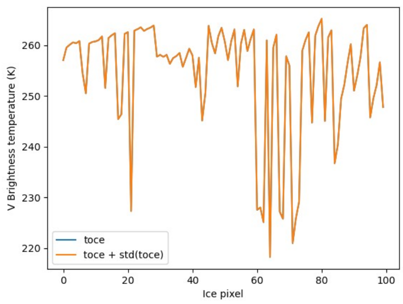

Sensitivity to s_{oce}

Ice type: “fresh ice”

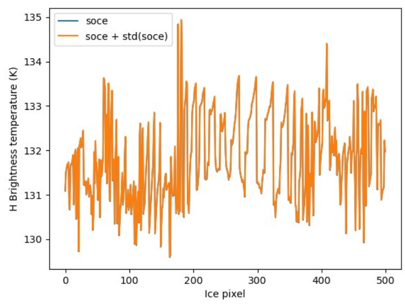

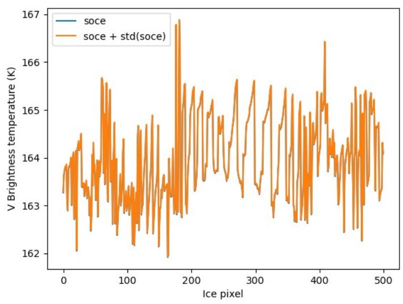

Ice type: “first-year ice”

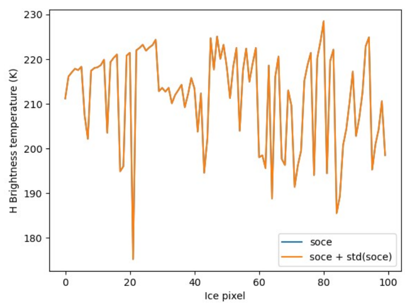

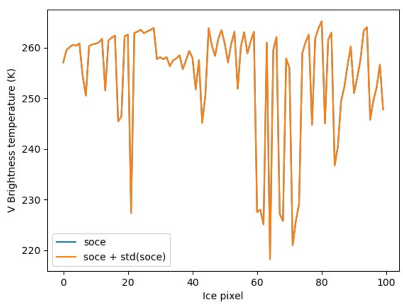

A4. Sensitivity studies: SMRT with AMSR2 10.65 GHz data

Sensitivity to *h_{snw}*

Ice type: “fresh ice”

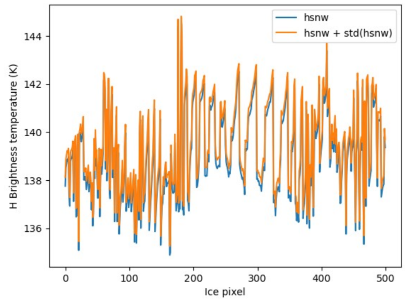

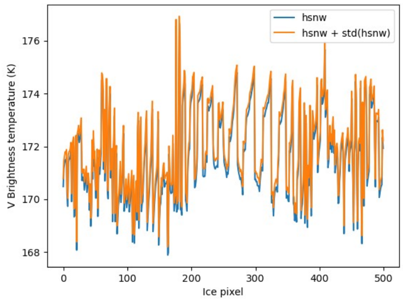

Ice type: “first-year ice”

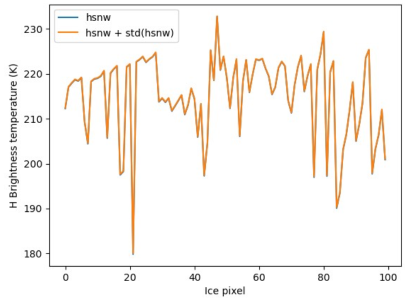

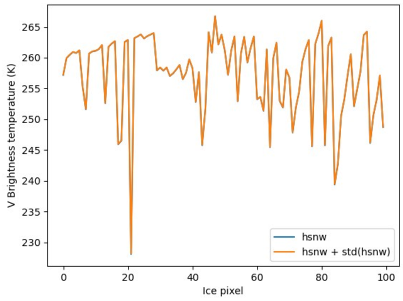

Sensitivity to *t_{snw}*

Ice type: “fresh ice”

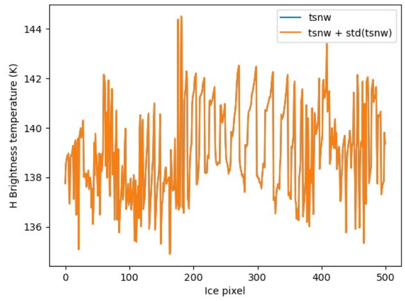

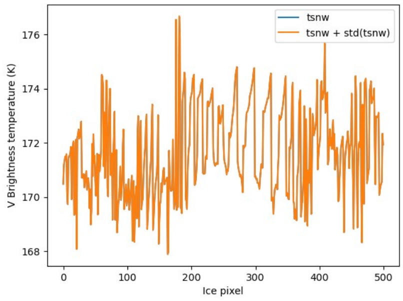

Ice type: “first-year ice”

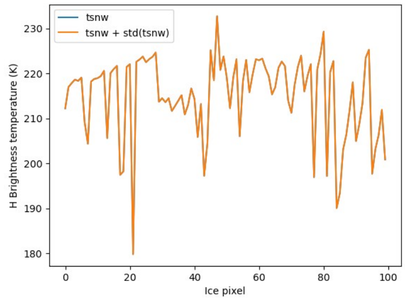

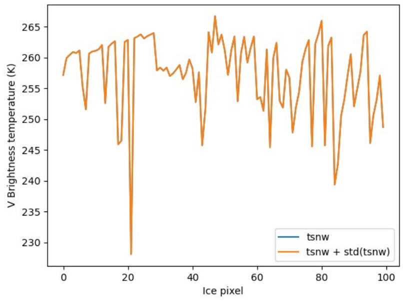

Sensitivity to d_{snw}

Ice type: “fresh ice”

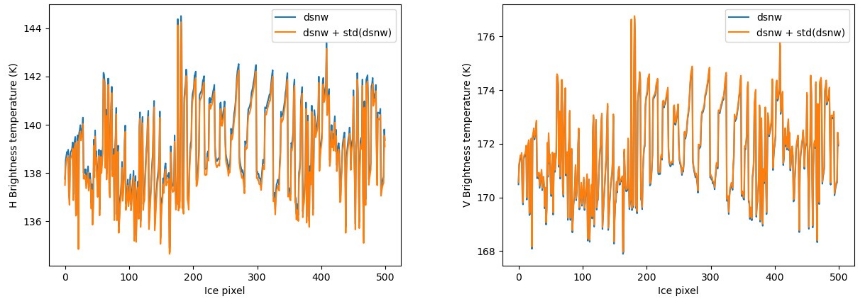

Ice type: “first-year ice”

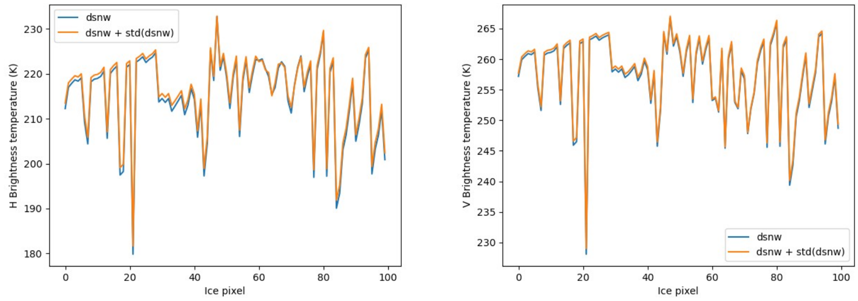

Sensitivity to l_{snw}

Ice type: “fresh ice”

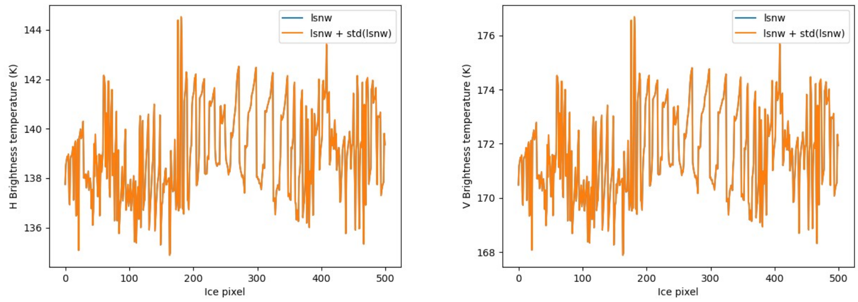

Ice type: “first-year ice”

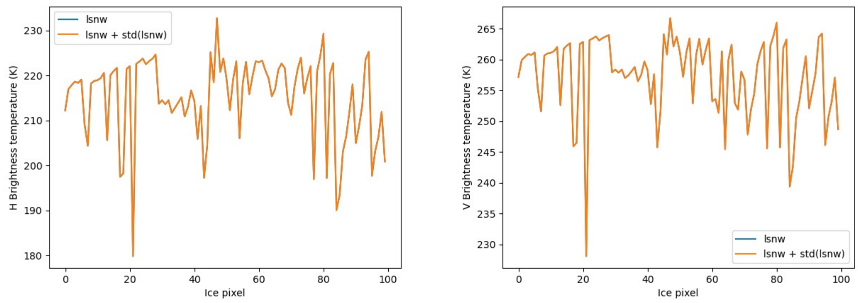

Sensitivity to h_{ice}

Ice type: “fresh ice”

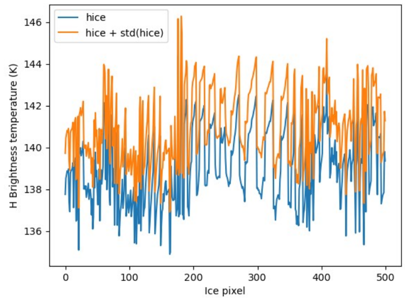

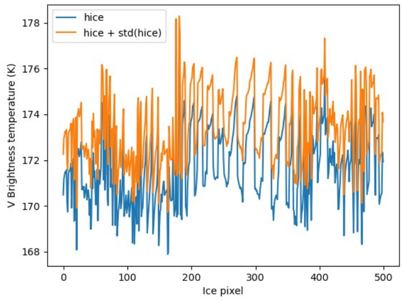

Ice type: “first-year ice”

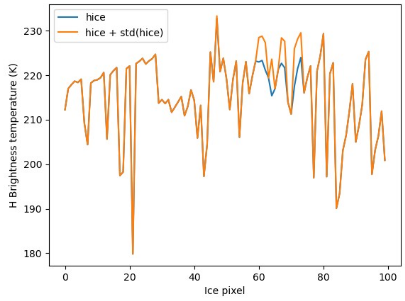

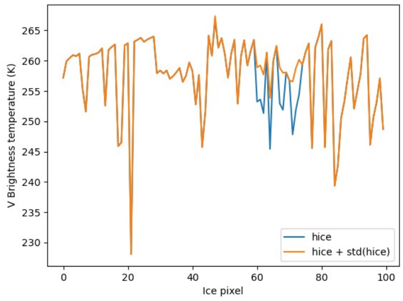

Sensitivity to t_{ice}

Ice type: “fresh ice”

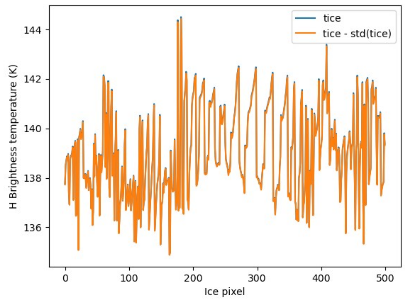

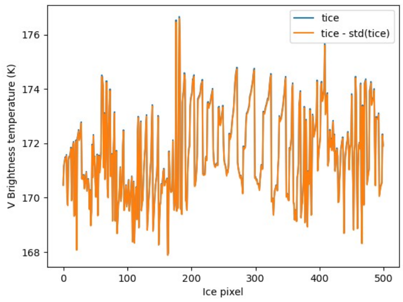

Ice type: “first-year ice”

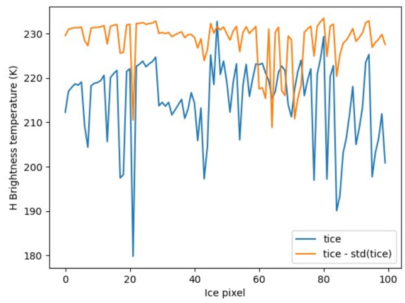

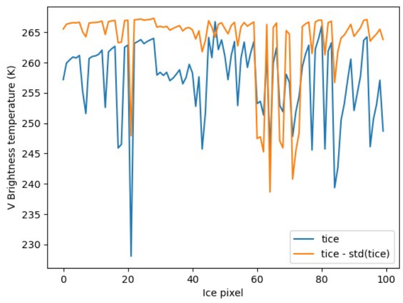

Sensitivity to s_{ice}

Ice type: “fresh ice”

(not applicable) (not applicable)

Ice type: “first-year ice”

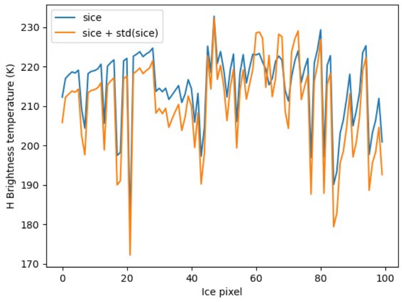

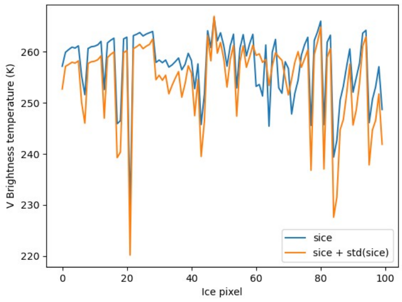

Sensitivity to r_{ice}

Ice type: “fresh ice”

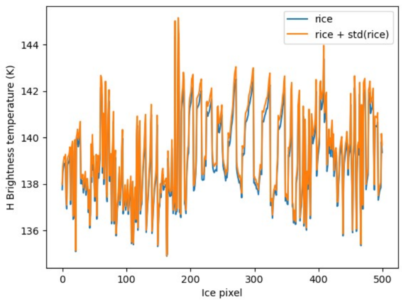

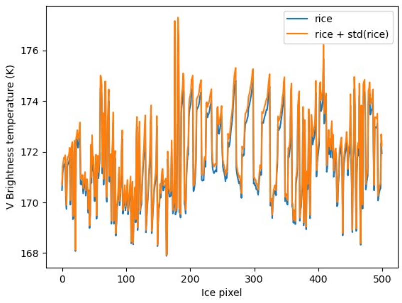

Ice type: “first-year ice”

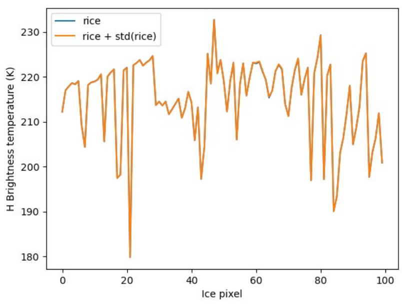

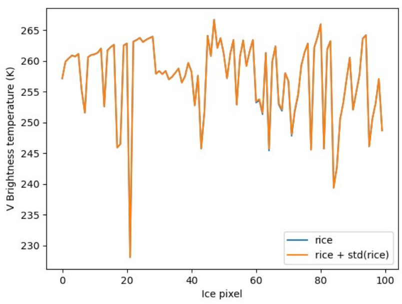

Sensitivity to p_{ice}

Ice type: “fresh ice”

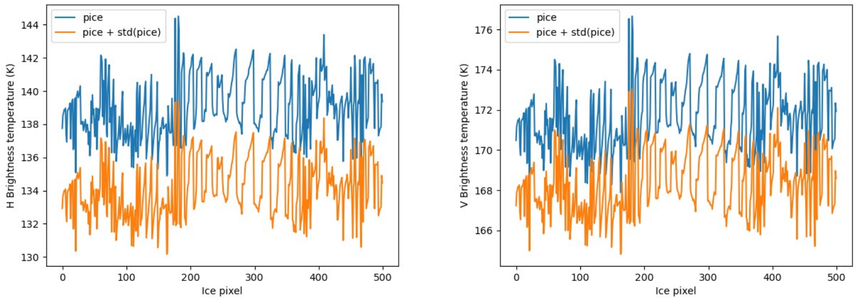

Ice type: “first-year ice”

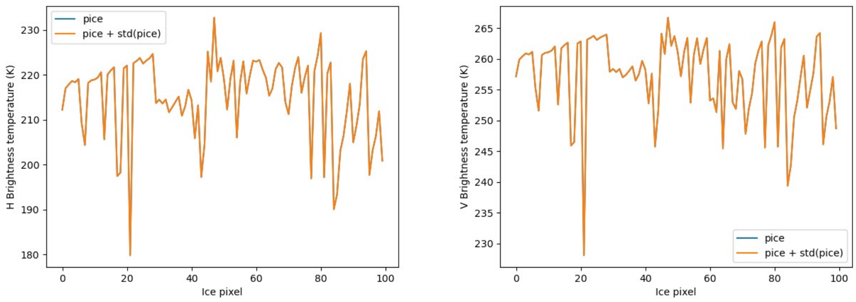

Sensitivity to ice type

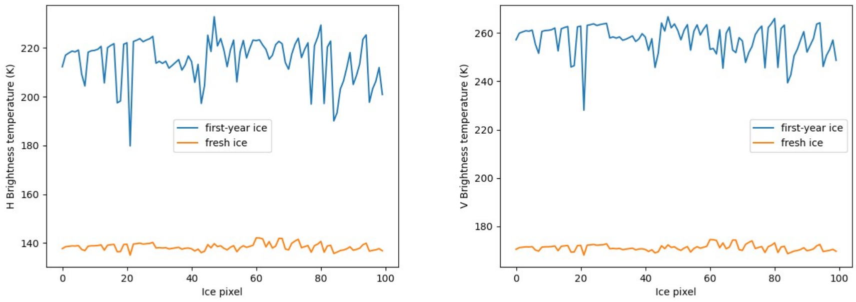

Sensitivity to t_{oce}

Ice type: “fresh ice”

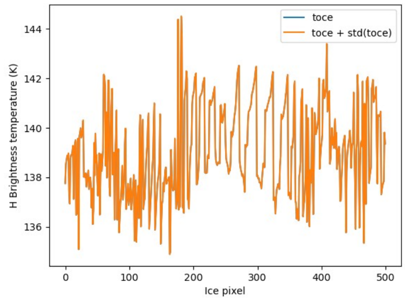

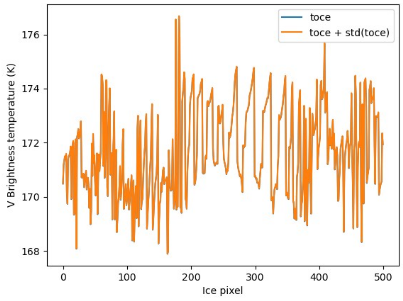

Ice type: “first-year ice”

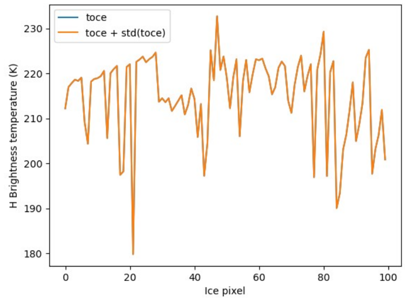

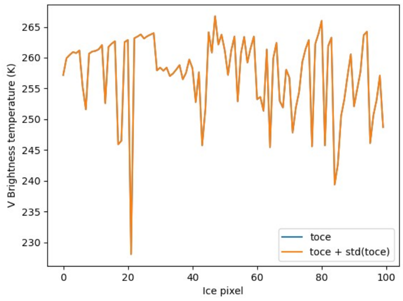

Sensitivity to s_{oce}

Ice type: “fresh ice”

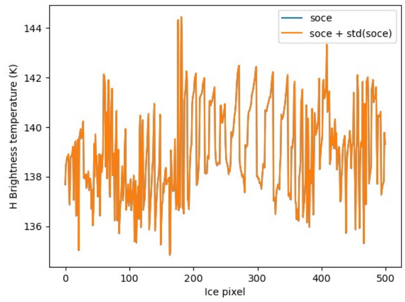

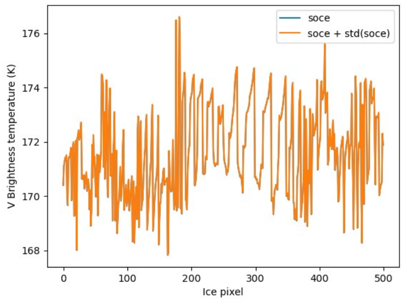

Ice type: “first-year ice”

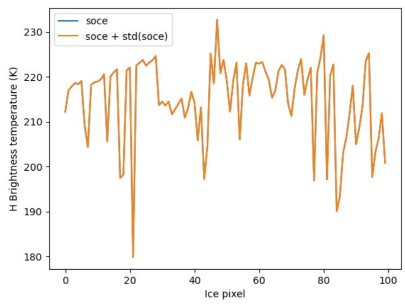

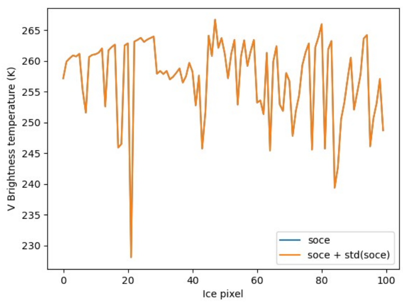

A5. Sensitivity studies: SMRT with AMSR2 18.7 GHz data

Sensitivity to *h_{snw}*

Ice type: “fresh ice”

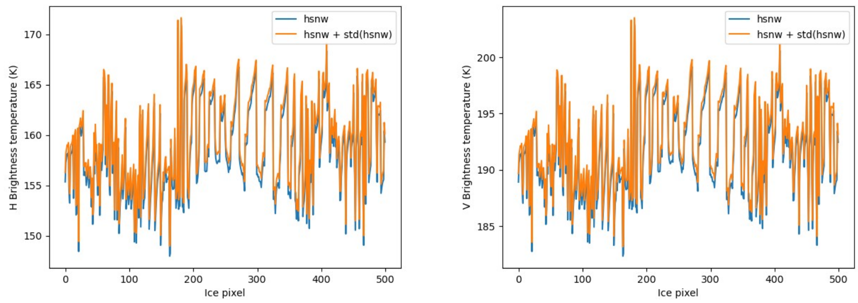

Ice type: “first-year ice”

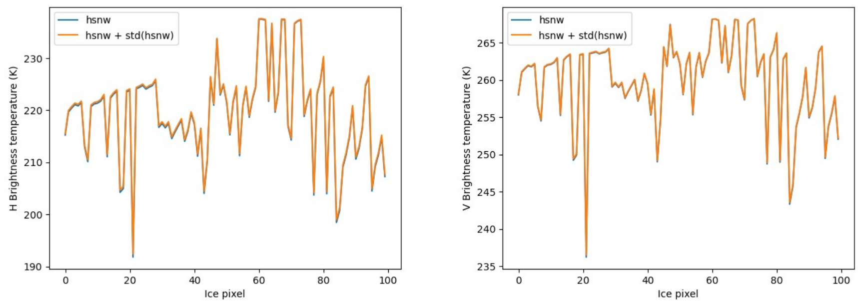

Sensitivity to *t_{snw}*

Ice type: “fresh ice”

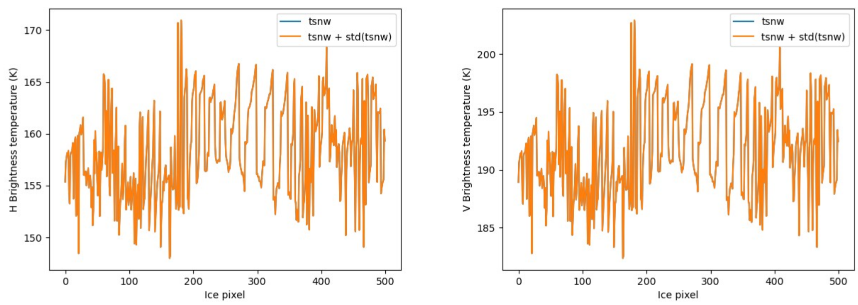

Ice type: “first-year ice”

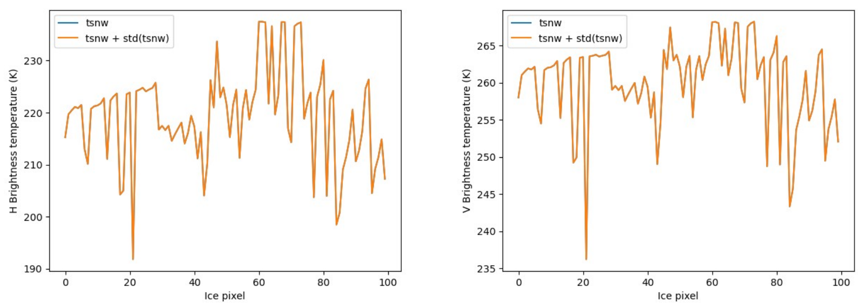

Sensitivity to d_{snw}

Ice type: “fresh ice”

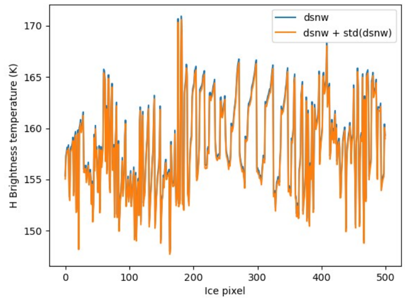

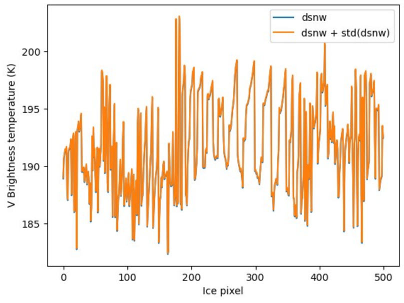

Ice type: “first-year ice”

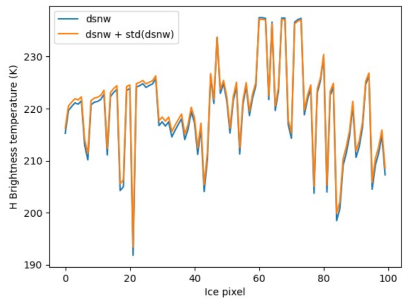

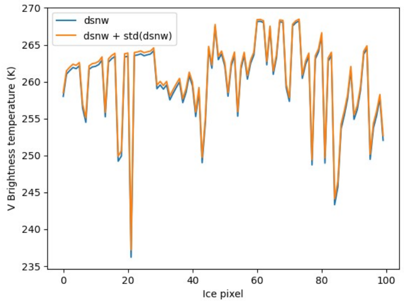

Sensitivity to l_{snw}

Ice type: “fresh ice”

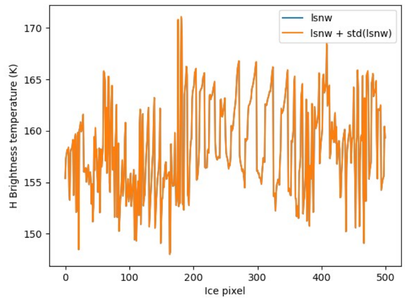

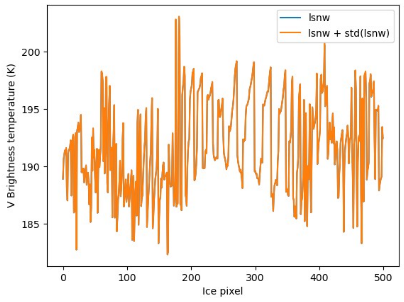

Ice type: “first-year ice”

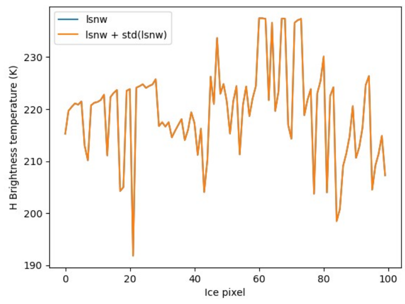

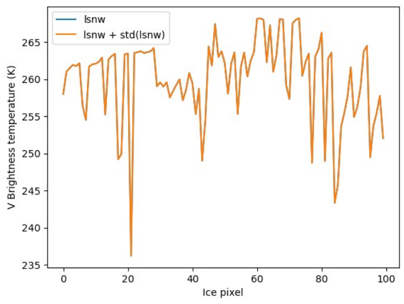

Sensitivity to h_{ice}

Ice type: “fresh ice”

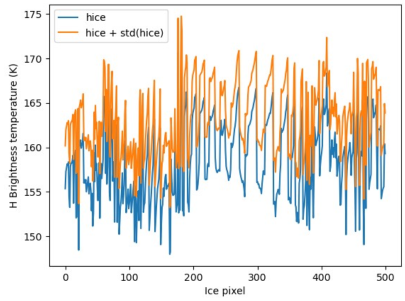

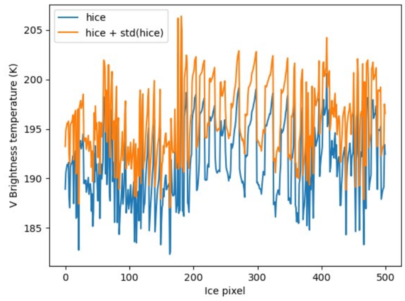

Ice type: “first-year ice”

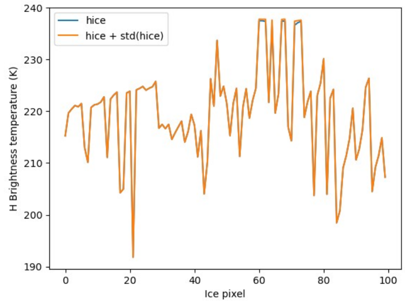

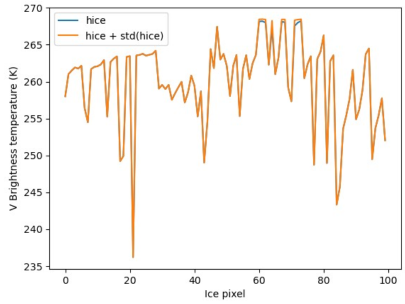

Sensitivity to t_{ice}

Ice type: “fresh ice”

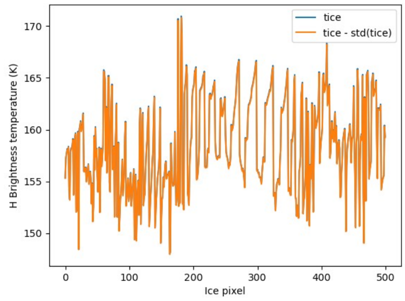

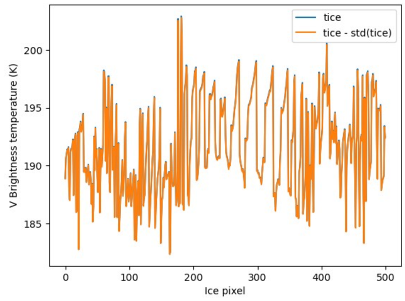

Ice type: “first-year ice”

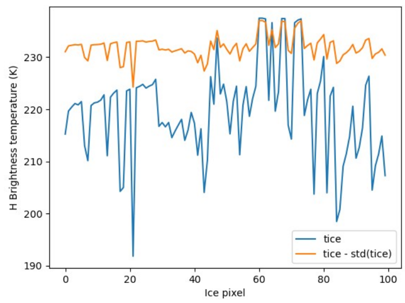

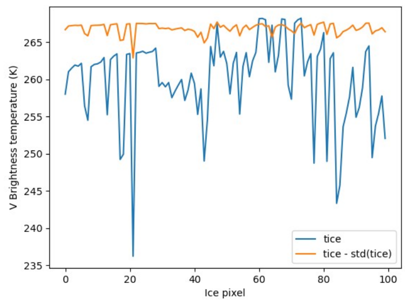

Sensitivity to s_{ice}

Ice type: “fresh ice”

(not applicable) (not applicable)

Ice type: “first-year ice”

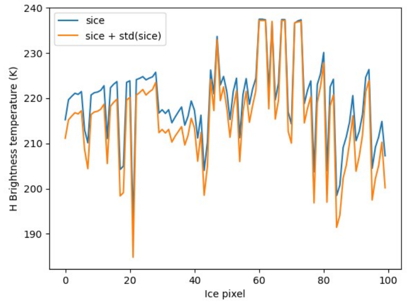

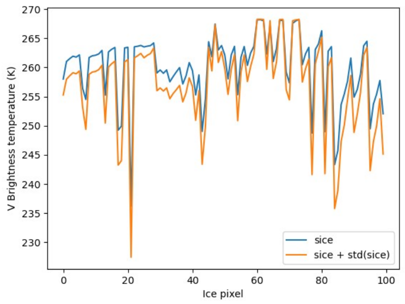

Sensitivity to r_{ice}

Ice type: “fresh ice”

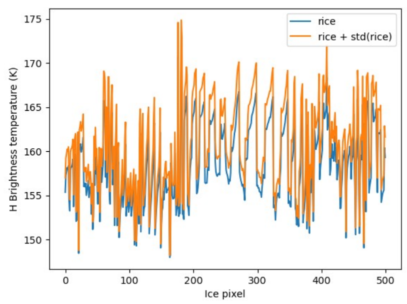

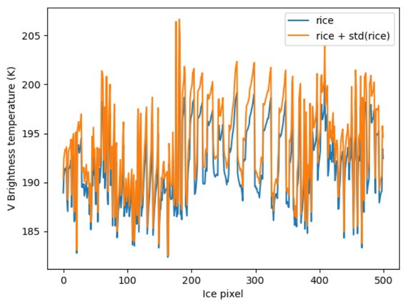

Ice type: “first-year ice”

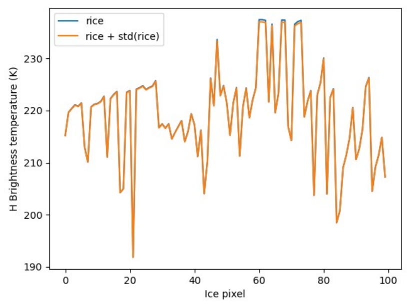

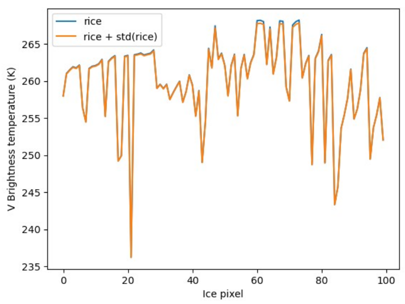

Sensitivity to p_{ice}

Ice type: “fresh ice”

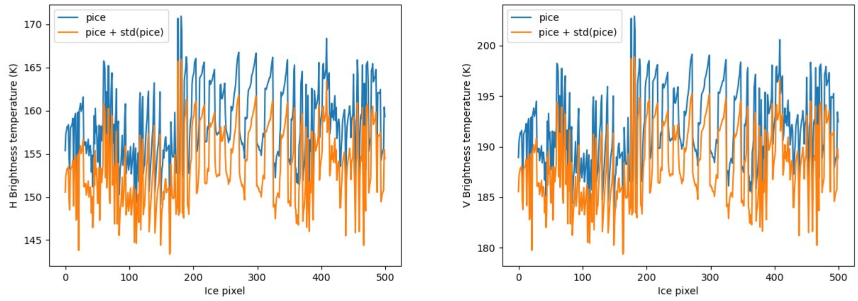

Ice type: “first-year ice”

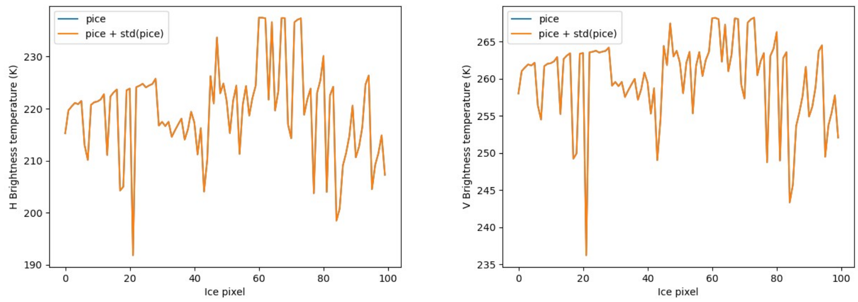

Sensitivity to ice type

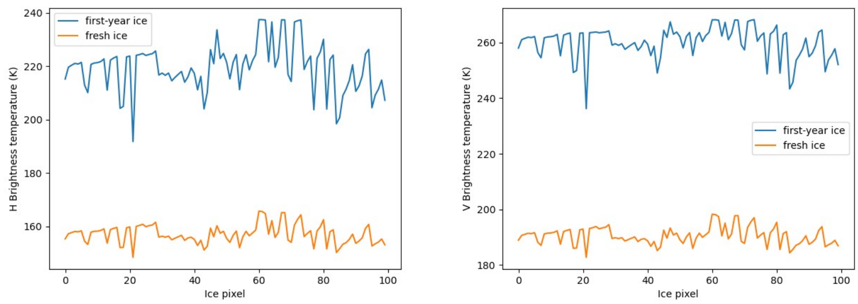

Sensitivity to t_{oce}

Ice type: “fresh ice”

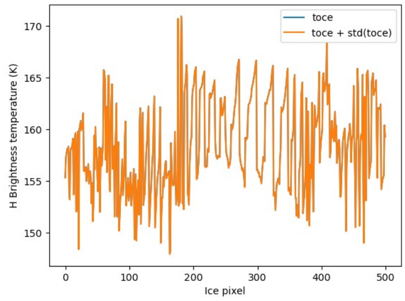

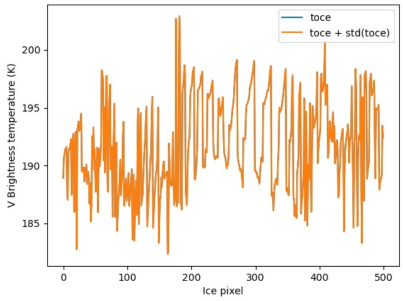

Ice type: “first-year ice”

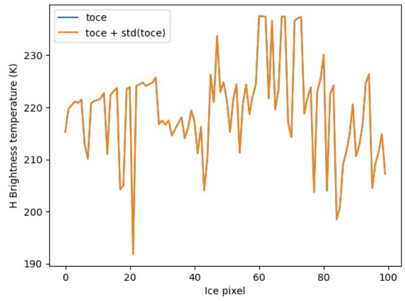

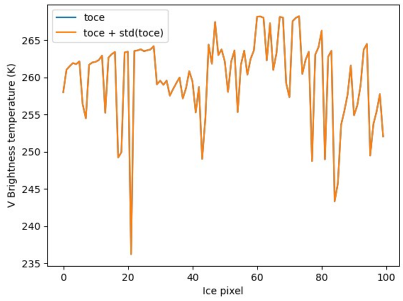

Sensitivity to s_{oce}

Ice type: “fresh ice”

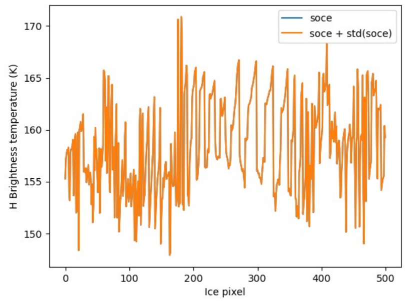

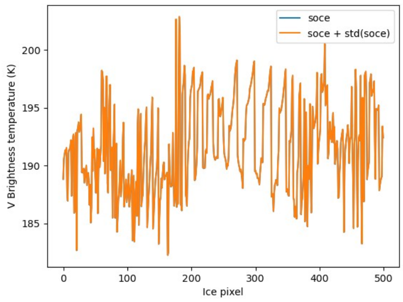

Ice type: “first-year ice”

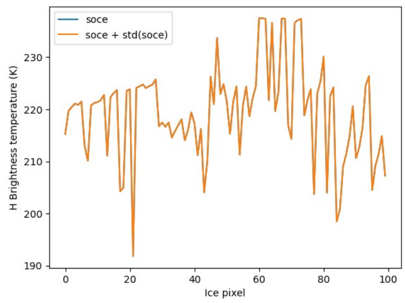

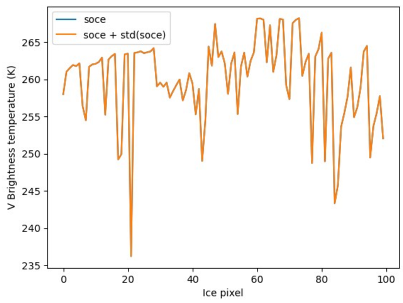

A6. Sensitivity studies: SMRT with AMSR2 36.5 GHz data

Sensitivity to h_{snw}

Ice type: “fresh ice”

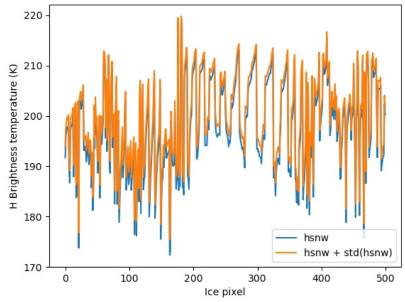

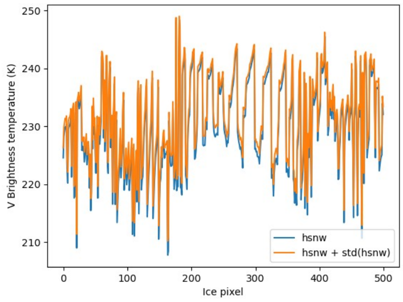

Ice type: “first-year ice”

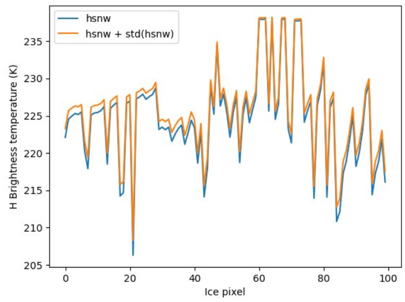

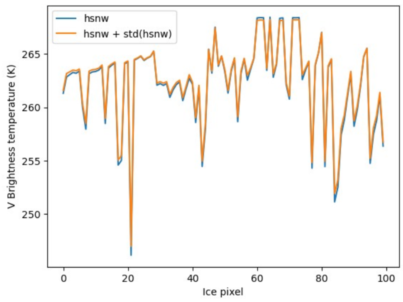

Sensitivity to t_{snw}

Ice type: “fresh ice”

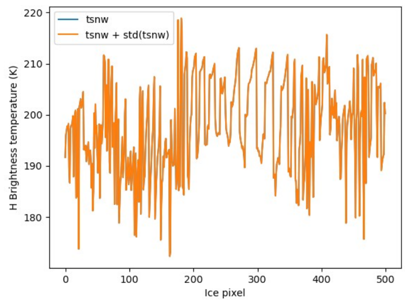

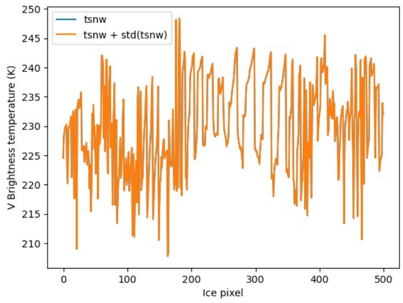

Ice type: “first-year ice”

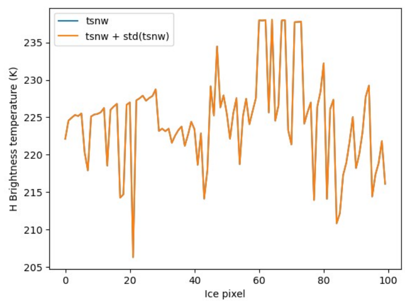

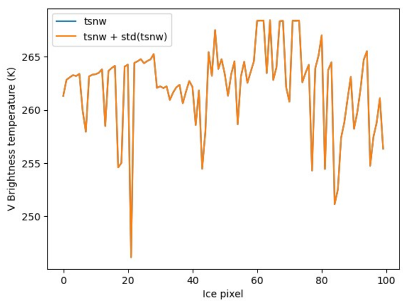

Sensitivity to d_{snw}

Ice type: “fresh ice”

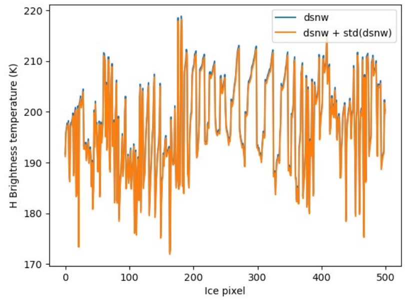

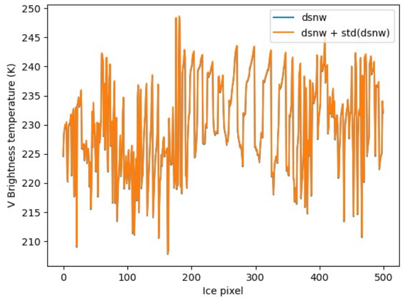

Ice type: “first-year ice”

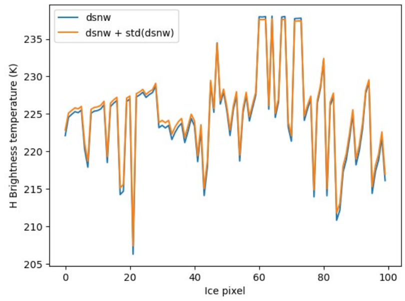

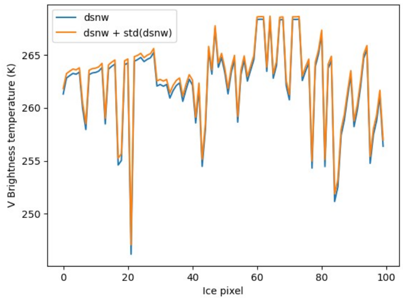

Sensitivity to l_{snw}

Ice type: “fresh ice”

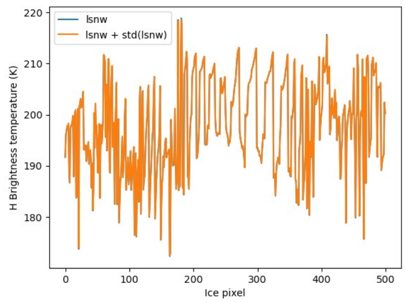

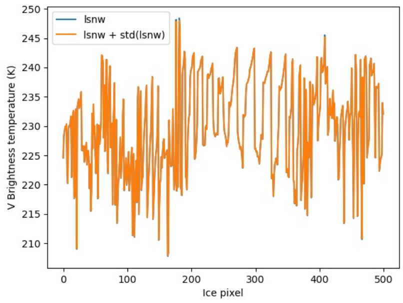

Ice type: “first-year ice”

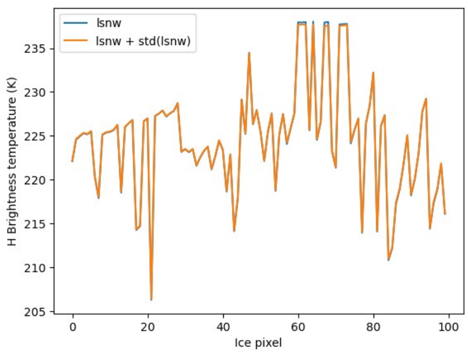

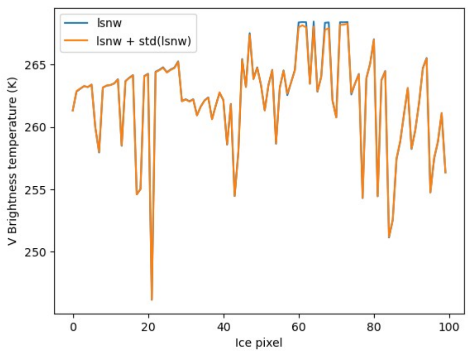

Sensitivity to h_{ice}

Ice type: "fresh ice"

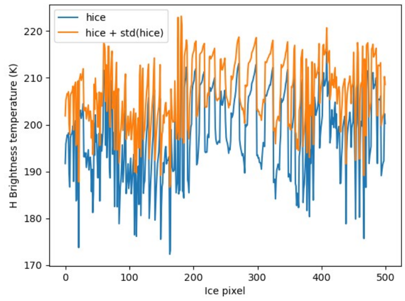

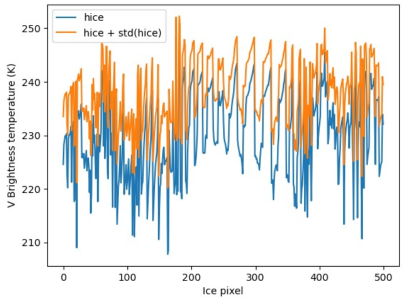

Ice type: "first-year ice"

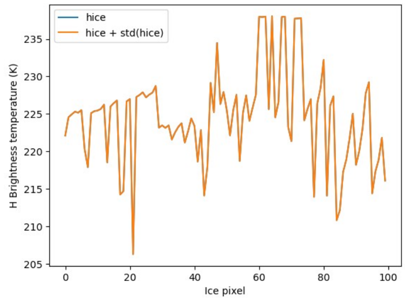

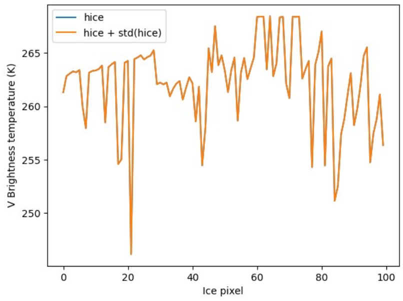

Sensitivity to t_{ice}

Ice type: "fresh ice"

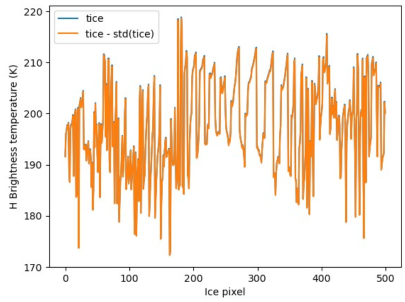

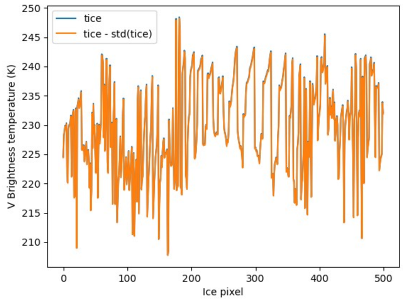

Ice type: "first-year ice"

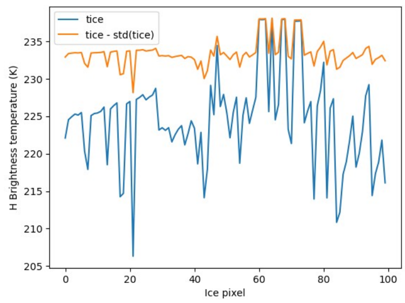

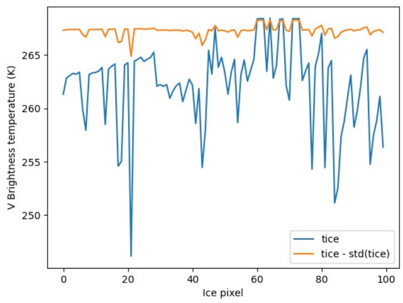

Sensitivity to s_{ice}

Ice type: “fresh ice”

(not applicable) (not applicable)

Ice type: “first-year ice”

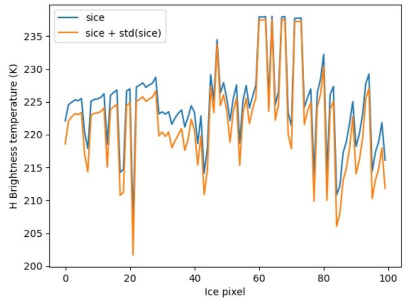

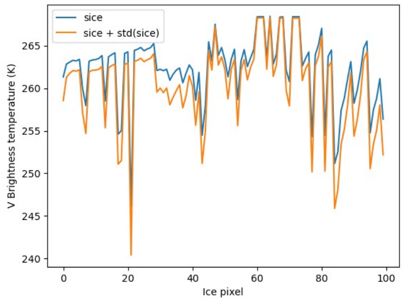

Sensitivity to r_{ice}

Ice type: “fresh ice”

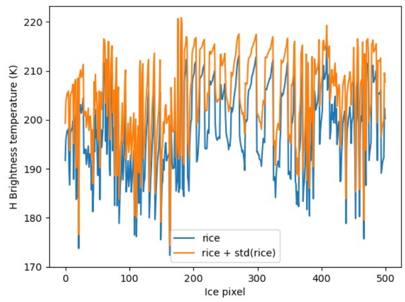

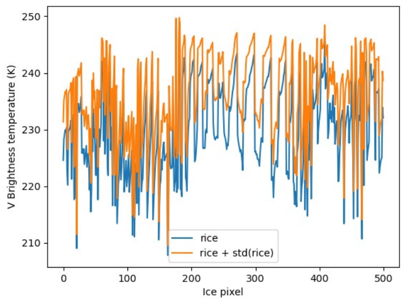

Ice type: “first-year ice”

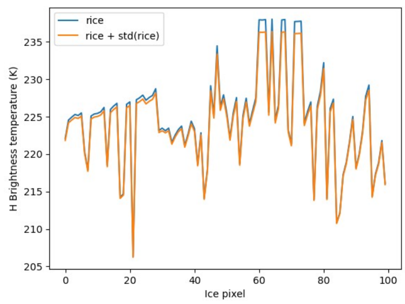

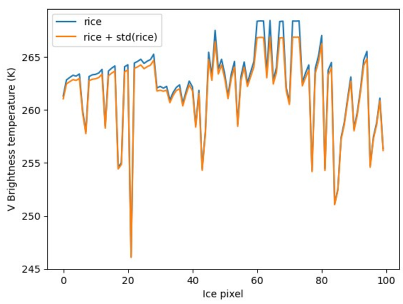

Sensitivity to p_{ice}

Ice type: “fresh ice”

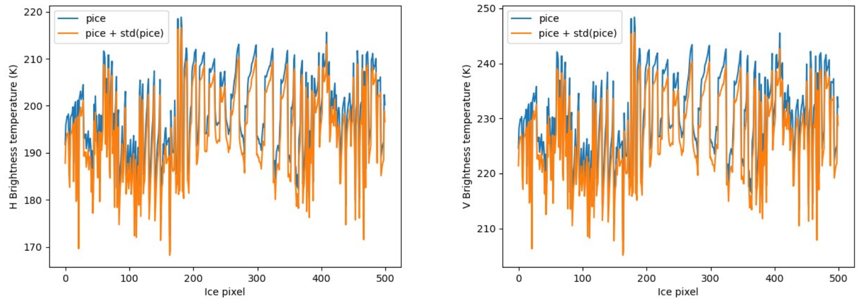

Ice type: “first-year ice”

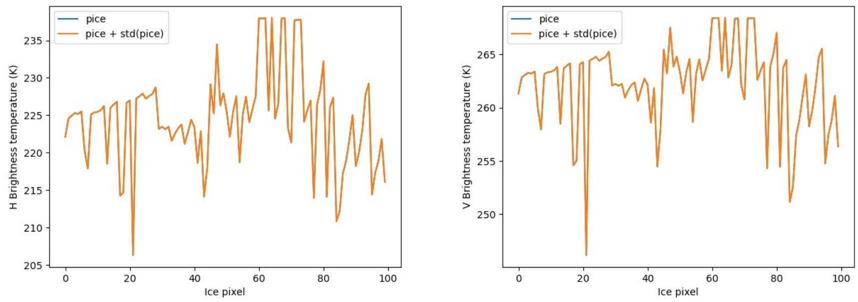

Sensitivity to ice type

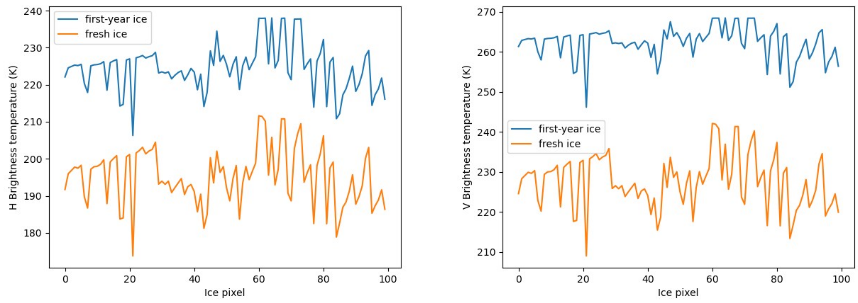

Sensitivity to t_{oce}

Ice type: “fresh ice”

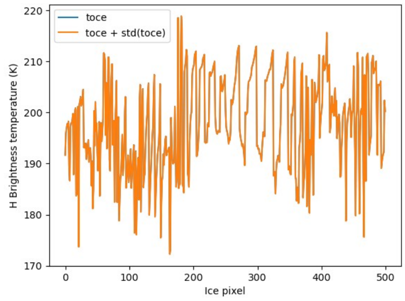

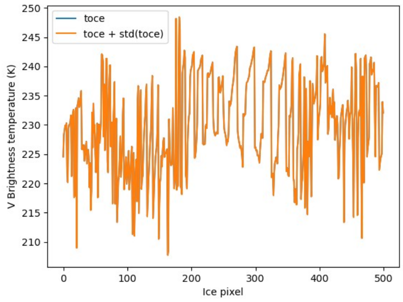

Ice type: “first-year ice”

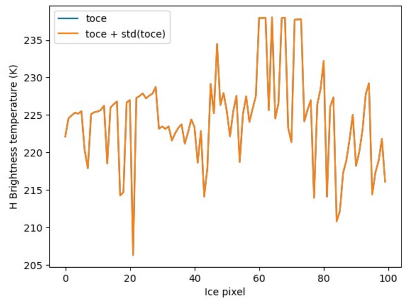

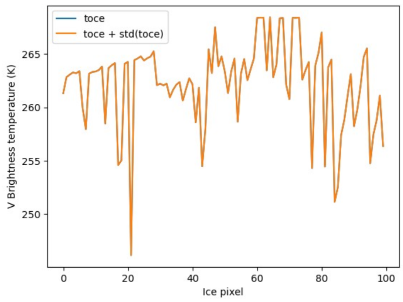

Sensitivity to s_{oce}

Ice type: “fresh ice”

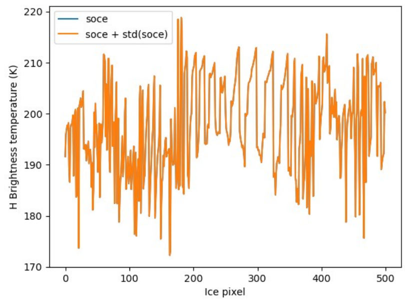

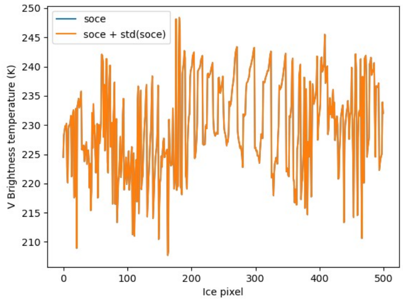

Ice type: “first-year ice”

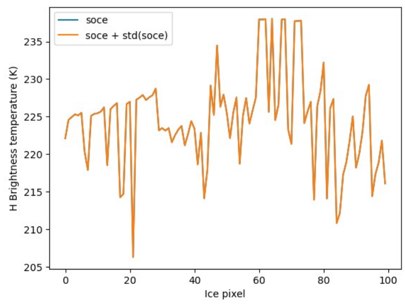

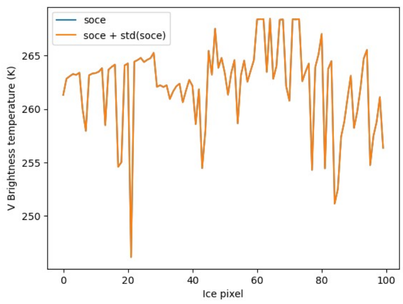

A7. Histograms for model minus observations (AMSR2)

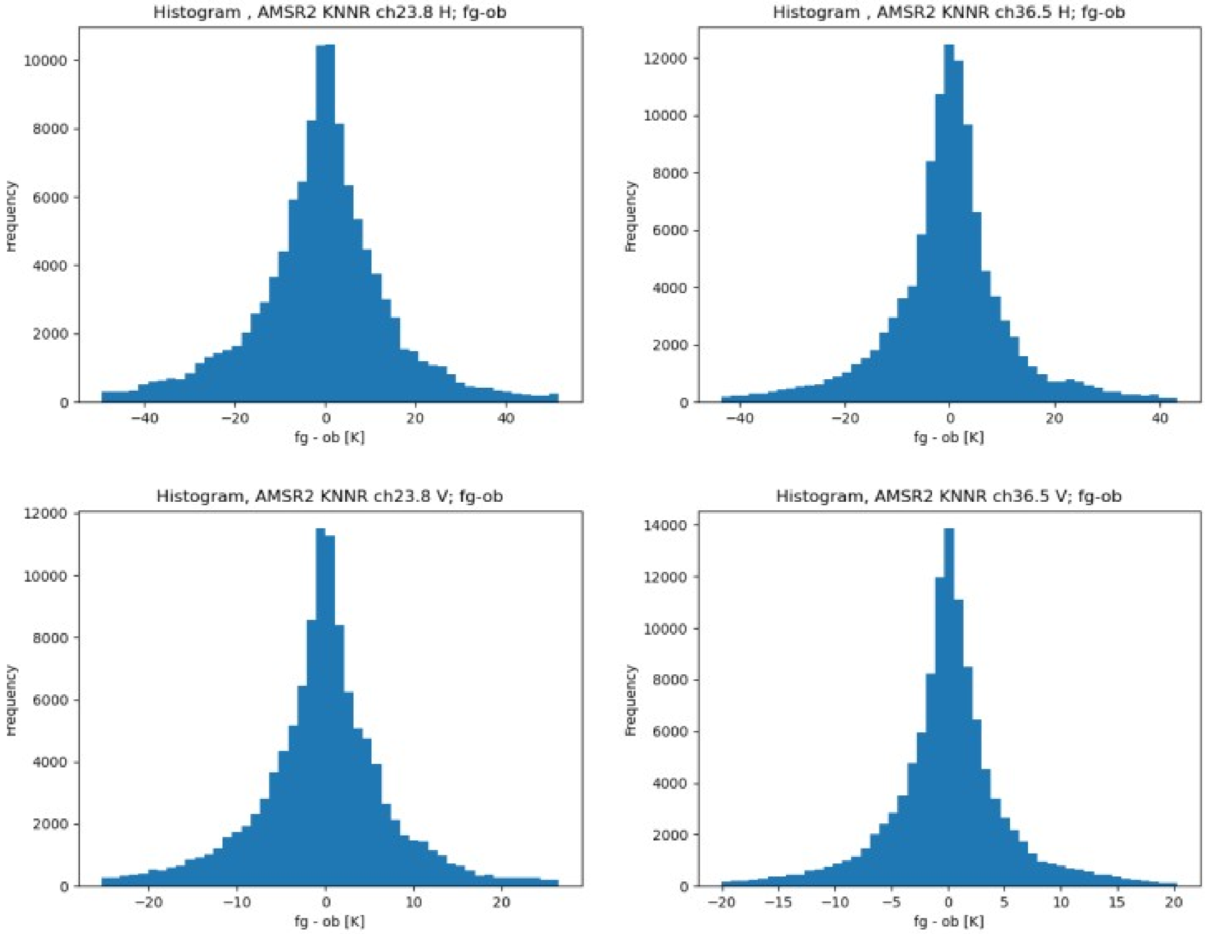

Figure A7.1. Histogram for differences between KNNR modelled (fg) and observed (ob) brightness temperatures from AMSR2 channels at 23.8 GHz (left) and 36.5 GHz (right) for horizontal (top) and vertical (bottom) polarizations. All data from Dec 2016 - May 2017.

A8. Density plots for observed and modelled AMSR2 channels

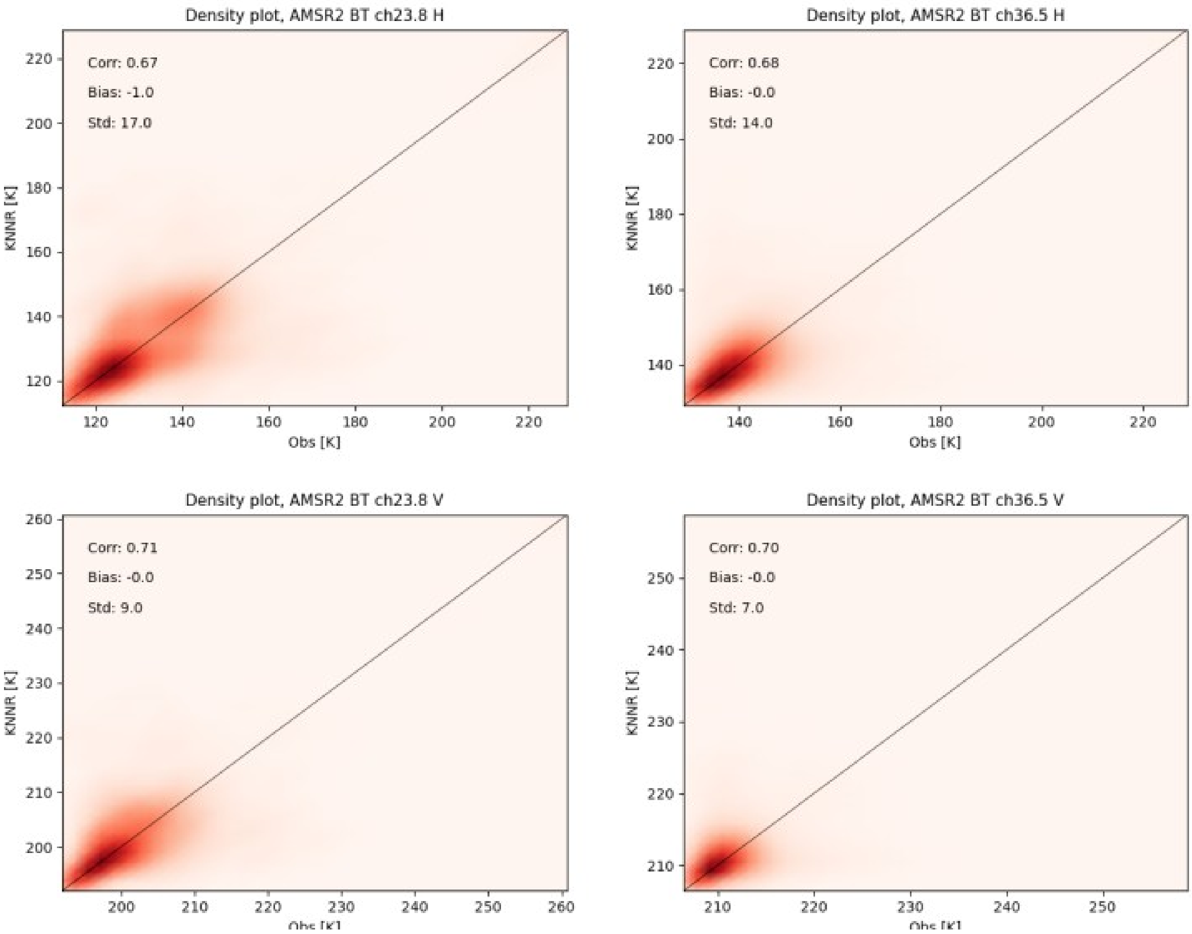

Figure A8.1. Density plots for observed (x-axis) and KNNR modelled (y-axis) brightness temperatures for AMSR2 channels at 23.8 GHz (left) and 36.5 GHz (right) for horizontal (top) and vertical (bottom) polarizations. Data from Dec 2016 - May 2017.

A9. Examples of AMSR2 data for the date 2017-02-11:02 UTC

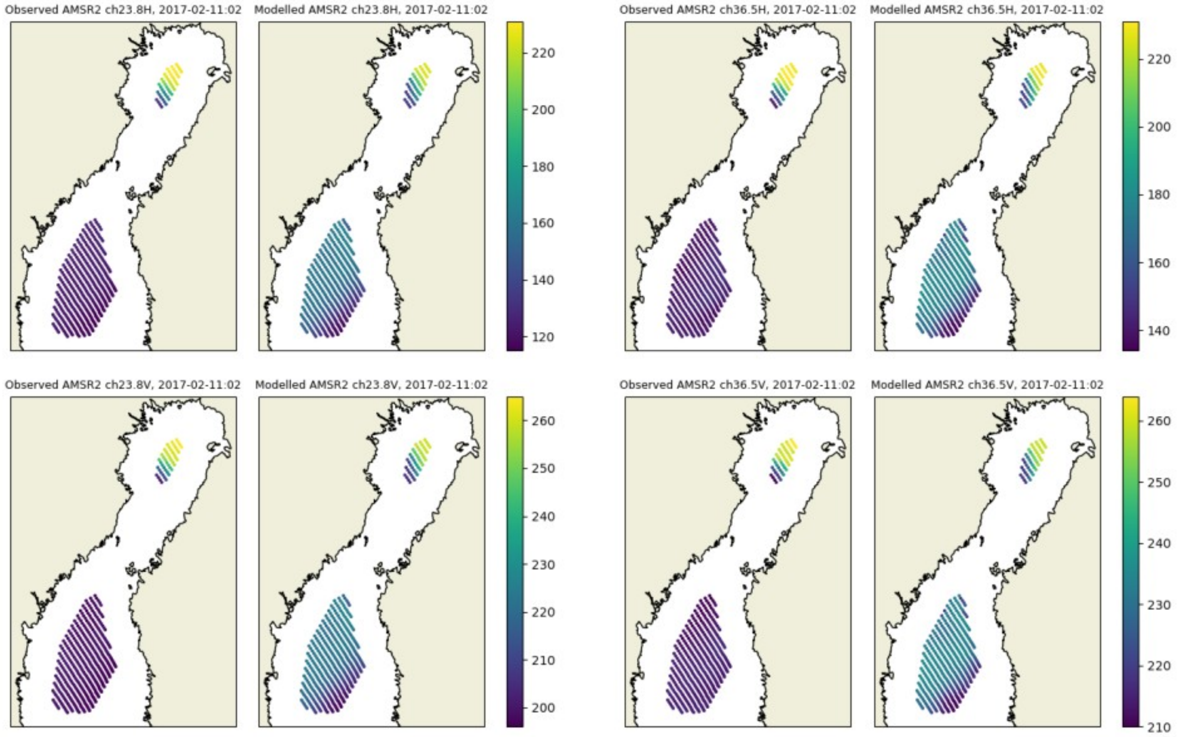

Figure A9.1. Observed (1st and 3rd columns) and modelled (2nd and 4th columns) AMSR2 brightness temperatures at 23.8 and 36.5 GHz for H (top) and V(bottom) polarizations.